

## CHAPTER 5

### INTERPRETATION OF CHLORIDE, ISOTOPE AND SUCTION DATA

#### 5.1 HAMILTON HILL: HOLES 4, 12, 18, 20, 21

##### 5.1.1 NOTES ON TIME-SERIES

The most extensive set of data for one site is that for the Margaret River flood plain at Hamilton Hill. Hole 12 is at the northern edge of the flood plain, but the remaining holes within about 50 m of each other, except perhaps for hole 21, as vehicle tracks and traces of previous holes were obliterated by the flood of March 1989, making location difficult. Judging from the lack of tracks we were the first to enter the area since that flood.

The examination of a time series of data from holes at the same site provides the best indication of whether the profiles are in steady-state or not, and hence the validity of the convection-diffusion model used to make evaporation estimates. Some idea of any seasonal variations, and the effect of extreme events (the flood of March 1989) is also gained.

The water content profiles of holes 4, 18, 20 and 21 are shown in figure 5.1.1a. Hole 12 is quite different and is omitted for clarity. The plot gives an indication of the similarity in lithology, with clayey layers holding more water than sandy layers. Holes 4, 18 and 20 are quite similar, while hole 21 is less comparable, being much sandier down to 1.7 m.

The chloride in soil solution profiles (Fig. 5.1.1b) of holes 4, 18, 20 and 21 are all similar below about 0.7 m, converging to nearly the

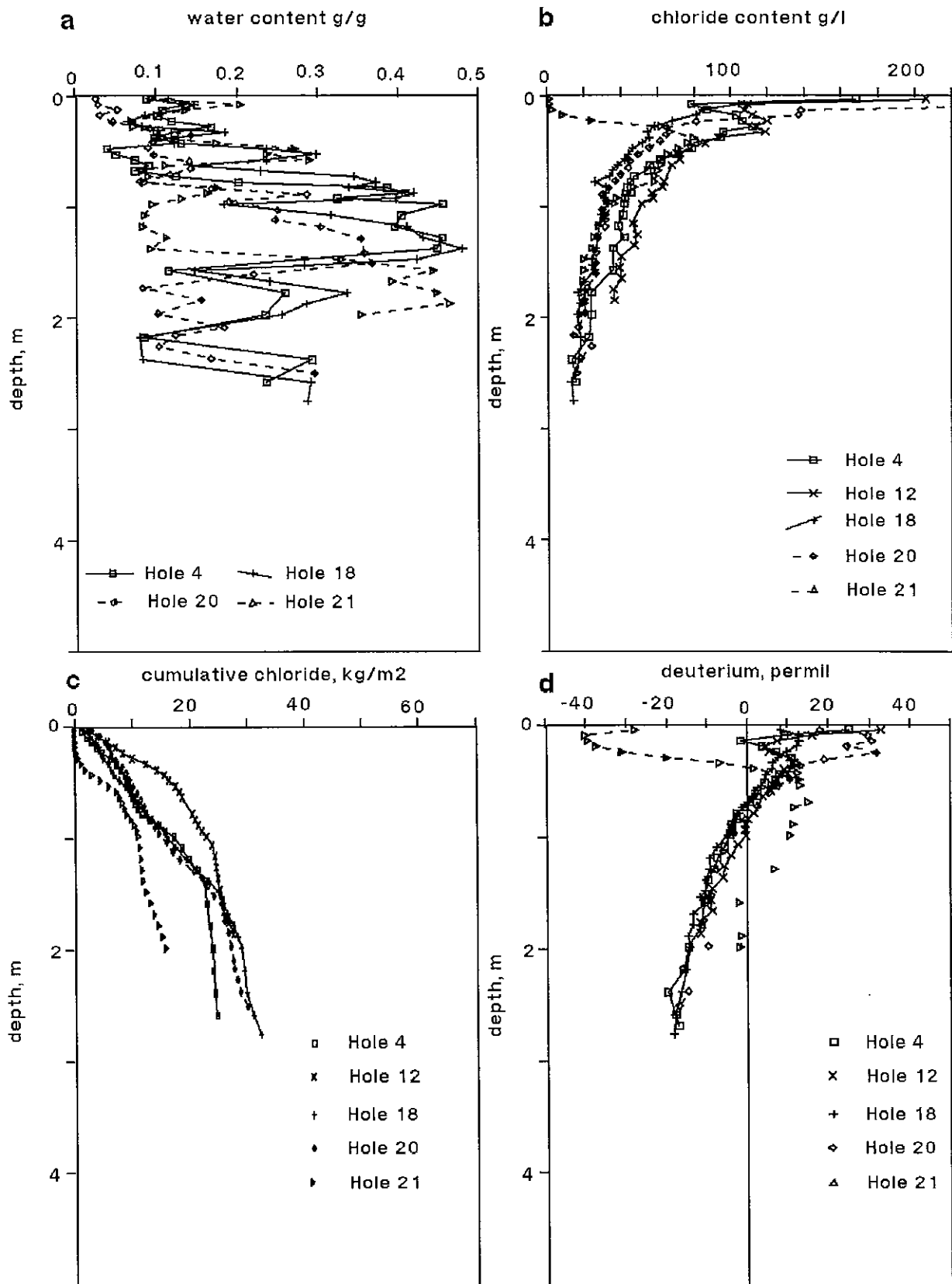


FIGURE 5.1.1 Profile comparisons, Hamilton Hill site

same value at the base. The build up of salt at the land surface between hole 4, after the above average winter 1986 rains, and hole 20, at the end of summer 1987, is quite apparent. The shape of the profile below about 0.7 m is mostly unaffected, even after the large March 1989 flood (hole 21), as may be taken to represent a long-term, close to steady-state situation.

Hole 12 shows a similar shape to the lower part of the Cl profile to the others, although the absolute values are higher, in keeping with the higher chlorinity of the shallow groundwater, 33 600 mg l<sup>-1</sup> compared to 16 300 to 22 500 mg l<sup>-1</sup>).

The flushing of the top part of the profile by the March 1989 flood is very evident in hole 21, but only extends to 0.4 m. The water in the profile above this depth amounts to 72 mm, and may represent the depth of water infiltrated during the event.

The amount of Cl present in the profiles is shown as cumulative chloride in kg m<sup>-2</sup> in figure 5.1.1c. There is an apparent build up of Cl evident in the lower parts of holes 18 and 20 over 4; this is probably just a reflection of the greater amount of water stored in the former over the latter, (0.91 m, 0.72 m and 0.46 m respectively, to depth 2.2m), which is due to higher average clay content. Hole 21 was sandier again, and contains less Cl, and the surface flushing is again apparent. Hole 12 contains more salt at shallow depths where it is fairly clayey and the chlorinity is high, and less at depth where sandy, so that the cumulative value falls to one similar to holes 18 and 20.

Deuterium profiles of holes 4, 12, 18 and 20 show a remarkable overlay below about 0.7 m, and diverge considerably above that (Fig. 5.1.1d). As with chloride, the deeper part of the profile would seem to reflect the long-term situation, and the surface part responds to seasonal events. The bottom part of hole 21 show a similar shape to the

rest, but is offset by about 10 or 12%; the reason for this is unclear, as the difference is significantly greater than the accuracy of the extraction method and mass spectrometer. The shallow groundwater has also been enriched compared to the earlier holes by about the same amount. One explanation is that the profile has been displaced downward by infiltration (piston flow), and the water table now consists of isotopically enriched water recharged by the event, with little or no mixing with the previous saturated zone water now beneath it. The low suction throughout the profile allow this possibility, and it is usual for the pressure front of increased recharge to move considerably faster than the chloride front (Jolly *et al.*, 1989; in their field study the ratio was between 2.5 and 4). However the lower part of the chloride profile is the same as the other holes and does not support that interpretation.

Holes 4, 12 and 21 show the effect of infiltration of isotopically light water, to 0.30, 0.30 and 0.45 m, with enrichment of the surface (0.00 -0.05 m) datum, presumably by re-evaporation. These depths are also observed in the chloride data. The effect in hole 21 is particularly pronounced. Hole 18 shows the single-maximum "classic" evaporation profile of Allison *et al.* (1983), and hole 20, after a summer of high evaporation, enrichment down to about 0.30 m.

Matric suction profiles are only available for holes 18, 20 and 21 (fig. 5.1.1e). Suction, like chloride and isotopes, is fairly constant below about 0.7m, with the scatter there probably attributable to inaccuracies inherent in the method, which appears to be somewhat texture dependent. It shows the effect of progressive drying between holes 18 and 20, and wetting up of the surface layers in hole 21.

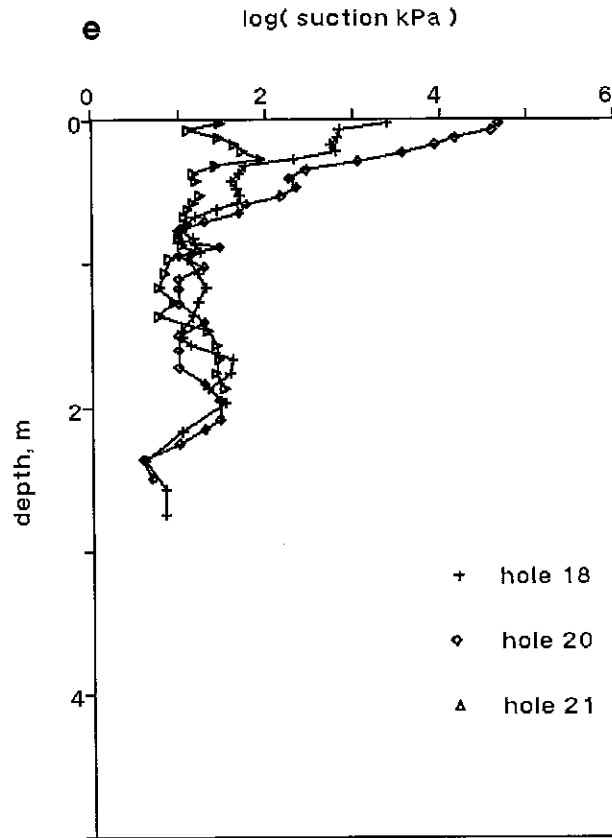


FIGURE 5.1.1 Profile comparisons, Hamilton Hill Site (continued)

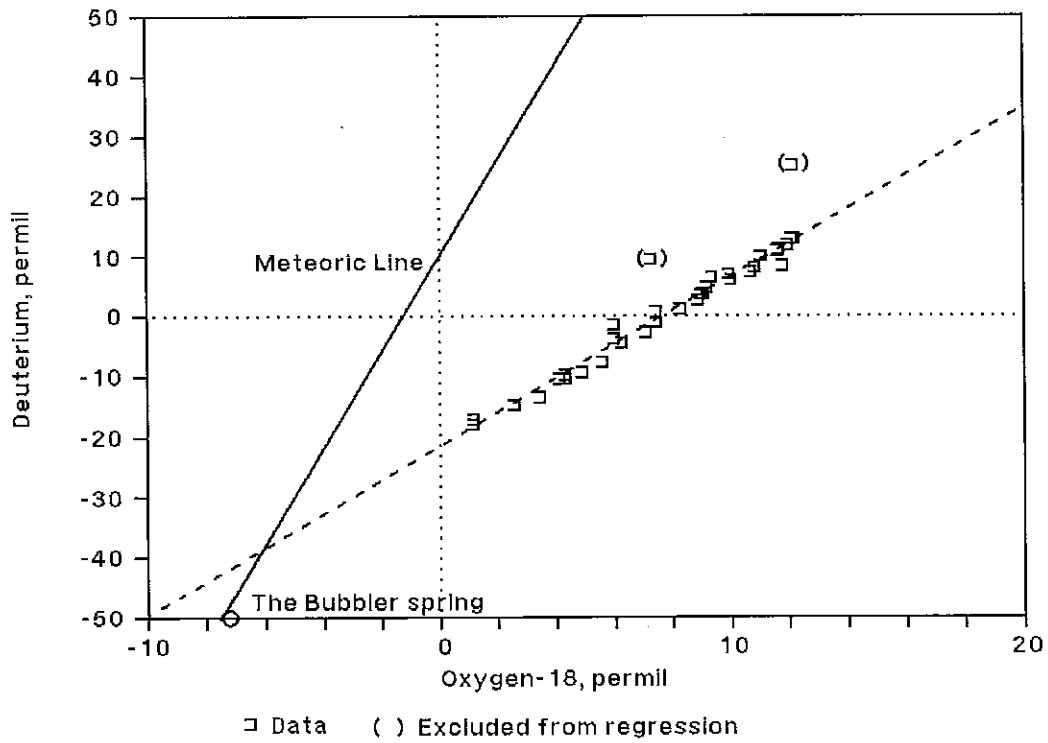


FIGURE 5.1.3 Hamilton Hill Site Pore Waters, O-18 - D Plot

### 5.1.2 EVAPORATION ESTIMATES

The constant character of the lower parts of the chloride and deuterium profiles from this site give confidence that the steady-state convection-diffusion model detailed in chapter 2 may be used to obtain estimates of evaporation from the field data. Plots of  $\ln(c-c_{res})$  against depth for holes 4, 12, 18 and 20 are given in figure 5.1.2. Note that the plots have been constructed for two possible bottom boundary conditions the concentration of solute in the shallow aquifer (marked res.= shallow) and deep, and lines of best fit are shown. For the purposes of linear regression on the logarithm-transformed data, the top few points have been excluded from all calculations, and the bottom few data as well for the "res.= shallow" calculations. The parameters required in the calculation of evaporation by  $E = -\theta_v f_1 D_0 \times \text{slope}$  are given in table 5.1.1., together with the slopes of the regression lines and standard error of those slopes (calculated using the Lotus 123 spreadsheet computer package). For the deep boundary condition, the errors in E due to the standard error of the slope are also given. These are in fact a minimum error in the result, because of the uncertainty of the parameters  $f_1$  (sections 2.2.4, 6.2.1), and  $\theta_v$ , estimated from a visual estimate of average  $\theta_g$  and an estimated average bulk density of  $1.6 \text{ Mg m}^{-3}$ . For the shallow boundary condition, E/D has been estimated from the nomogram (Fig. 2.3.2) without a specified error, and evaporation calculated from that ratio.

The estimates using deuterium, with the shallow reservoir boundary condition, are two to three times as high as those using chloride. Most of the difference is due to the higher impedance factor used in the former calculations. The estimates using the deep boundary condition are much closer to each other. The shallow reservoir boundary condition

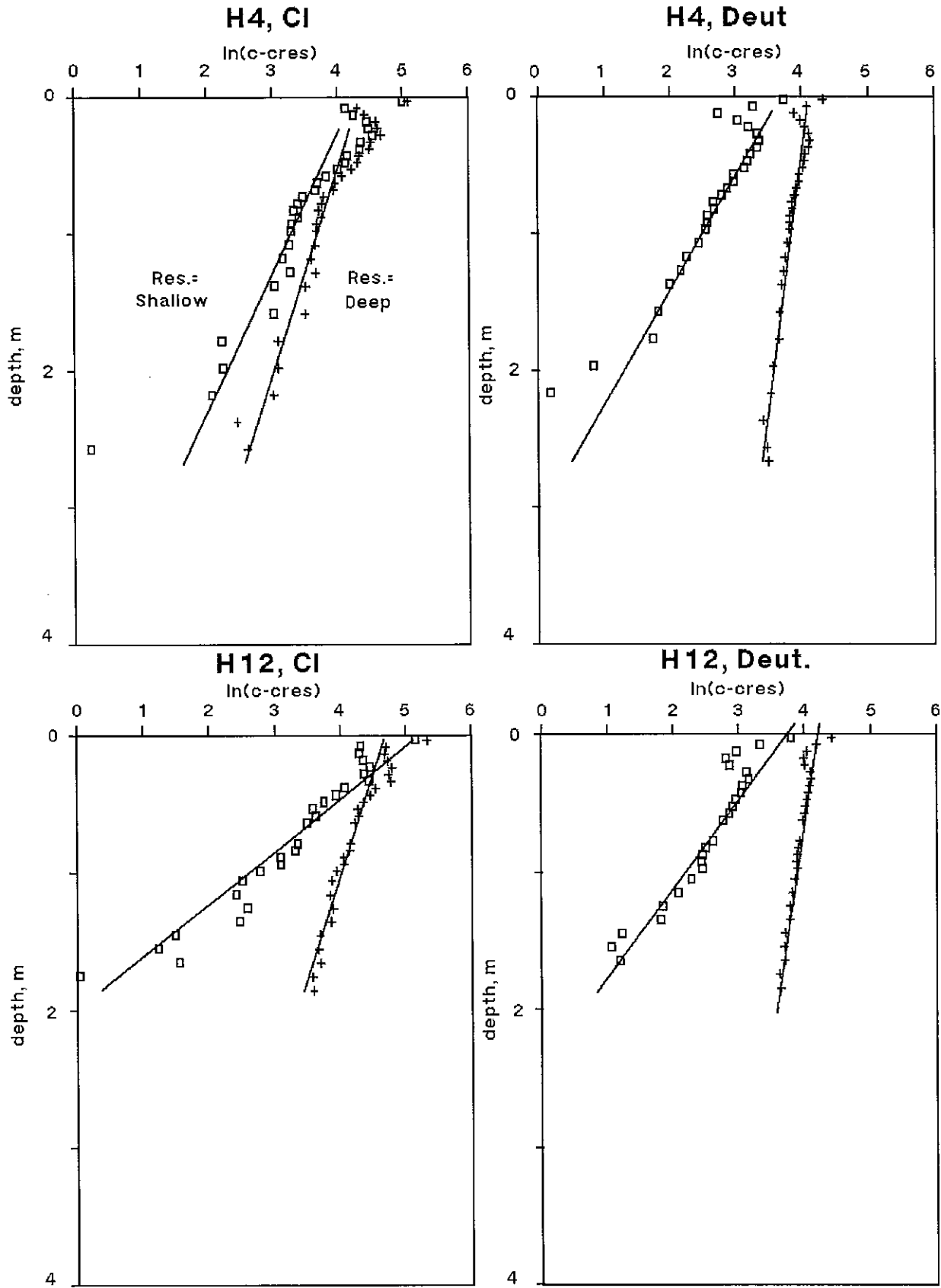


FIGURE 5.1.2 Holes 4 and 12  $\ln(C-Cres)$  vs Depth Plot

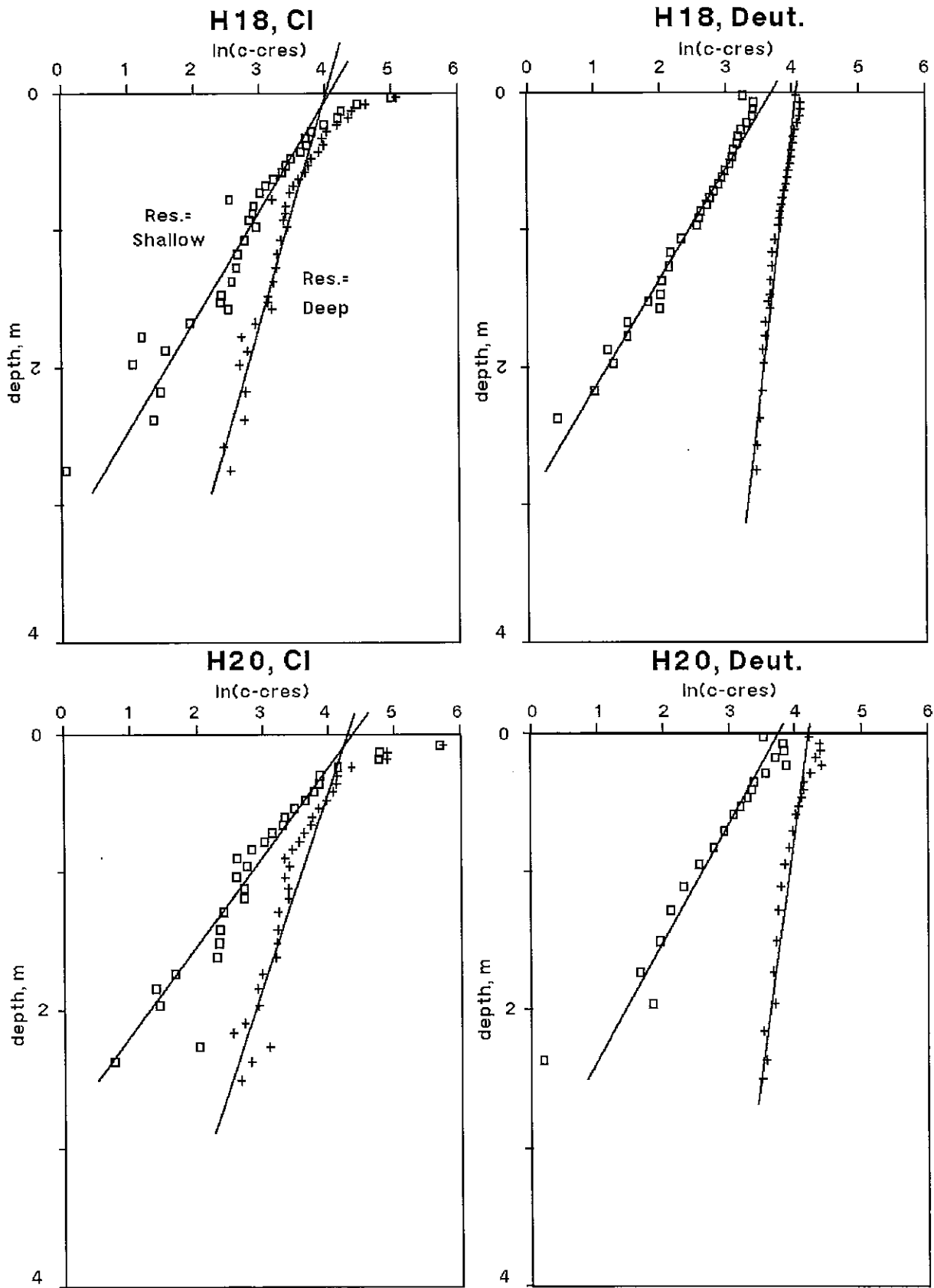


FIGURE 5.1.2 (cont.) Holes 18 and 20  $\ln(C-Cres)$  vs Depth Plots



TABLE 5.1.1

Evaporation Estimates, Hamilton Hill Site

a: General Parameters Used

Hole	Chloride		Deuterium
	$\theta_v$	$f_1$	$f_1$
		$D_0: 1.6 \times 10^{-9} \text{ m}^2 \text{ s}^{-1}$	$2.2 \times 10^{-9} \text{ m}^2 \text{ s}^{-1}$
4	0.40	0.27	0.5
12	0.26	0.16	0.5
18	0.48	0.33	0.5
20	0.30	0.19	0.5

b: Evaporation Estimates, Chloride

Hole	Shallow Reservoir			Deep Reservoir	
	Slope $\text{m}^{-1}$	E/D $\text{m}^{-1}$	Evaporation $\text{mm yr}^{-1}$	Slope $\text{m}^{-1}$	Evaporation $\text{mm yr}^{-1}$
4	$-0.972 \pm 0.097$	0.25	1.4	$-0.670 \pm 0.053$	$3.7 \pm 0.3$
12	$-2.694 \pm 0.218$	2.4	5.0	$-0.668 \pm 0.047$	$1.4 \pm 0.1$
18	$-1.242 \pm 0.079$	0.80	6.5	$-0.604 \pm 0.034$	$5.0 \pm 0.3$
20	$-1.535 \pm 0.089$	1.15	3.3	$-0.713 \pm 0.058$	$2.1 \pm 0.2$

TABLE 5.1.1 (Continued)

## Evaporation Estimates, Hamilton Hill Site

## c: Evaporation Estimates, Deuterium

Hole	Shallow Reservoir			Deep Reservoir	
	Slope $m^{-1}$	E/D $m^{-1}$	Evaporation $mm\ yr^{-1}$	Slope $m^{-1}$	Evaporation $mm\ yr^{-1}$
4	$-1.183 \pm 0.039$	0.60	8.3	$-0.271 \pm 0.014$	$3.8 \pm 0.2$
12	$-1.564 \pm 0.080$	0.95	8.6	$-0.310 \pm 0.008$	$2.8 \pm 0.1$
18	$-1.250 \pm 0.033$	0.80	13.3	$-0.256 \pm 0.010$	$4.3 \pm 0.2$
20	$-1.162 \pm 0.072$	0.55	5.7	$-0.303 \pm 0.021$	$3.2 \pm 0.2$

seems at first more appropriate physically, as the water table at the site existed in all holes in a sandy, permeable layer of alluvium. Lateral movement is therefore possible, and the water in the shallow aquifer perhaps regarded as well mixed; this could not be checked by deeper holes at this site. The increase in heavy isotope content of the water table following the flood of March 1989 is one piece of evidence against a well mixed character. In a well mixed aquifer vertical diffusion is not the dominant mode of solute transport. However, the permeable layer is likely to be thin compared to the total thickness of the aquitard below and so may have only a small influence on the overall profile. If there were no lateral movement or additional sources of water and salt, the deep boundary condition would still be appropriate. The characteristic time of the profiles may be calculated for the deep boundary condition case only, using  $t = D_{eff} / E^2$ . They vary from 300 to 1100 years. In these time frames, occasional floods may well be "averaged out" and the profiles best considered controlled by water supply from the deep aquifer and evaporation alone.

The chloride and deuterium concentrations of the profiles do appear to continue to decrease towards the bottom of the hole, rather than reaching a near constant value above the water table. This implies that there is a return flux of salt and deuterium to the water table, and that the deep boundary condition is more appropriate. A further support for the deep boundary condition is the much closer correspondence of the estimates from chloride and deuterium compared to the shallow option.

Holes 18 and 20 have fairly well defined evaporation front peaks in deuterium content, so that evaporation may also be estimated from the depth of the front as described in section 2.3. Taking the depths to be 0.10 and 0.25 m respectively, the estimates are 10.5 and 4.5 mm yr<sup>-1</sup>. These compare fairly well with the other estimates.

### 5.1.3 OXYGEN-18 - DEUTERIUM RELATIONSHIPS

Oxygen-18 measurements were made on holes 4, 18 and 20. The profiles matched the pattern of deuterium and are not presented; rather, the available data are plotted on a  $\delta D - \delta^{18}O$  plot (Fig. 5.1.3, which followed Fig. 5.1.1). The data fall on a well defined line, except for the two most shallow samples from hole 4; these are considered affected by infiltration and omitted from the regression analysis of the data. This yielded a line

$$\delta D = 2.80 \delta^{18}O - 21.5 \quad R^2 = 0.986 \quad (5.1)$$

with a standard error for the slope of 0.06. The slope is similar to but lower than that established for all the shallow groundwater data (section 4.5.3.5, slope 3.8), and crosses the meteoric line a little above the average value for The Bubbler spring, the most representative deep groundwater from the site.

### 5.1.4 WATER VAPOUR FLUX ESTIMATES

The calculated relative humidity profiles of holes 18, 20 and 21 are given in figures 5.1.4 to 6. Fluxes have been calculated as per section 2.4 (equations 2.54, 2.55, 2.66) for holes 18 and 20 (Tab. 5.1.2).

These values fit in fairly well with the long-term convection-diffusion estimates that range from 3 to 13 mm yr<sup>-1</sup> depending on the boundary condition taken, and gives some additional confidence in the order of such calculations. The profiles also illustrates that there exists a low humidity gradient all the way to the water table, because of the high salinity of the water and the shape of the chloride (salt)

# Hole 18 depth vs relative humidity

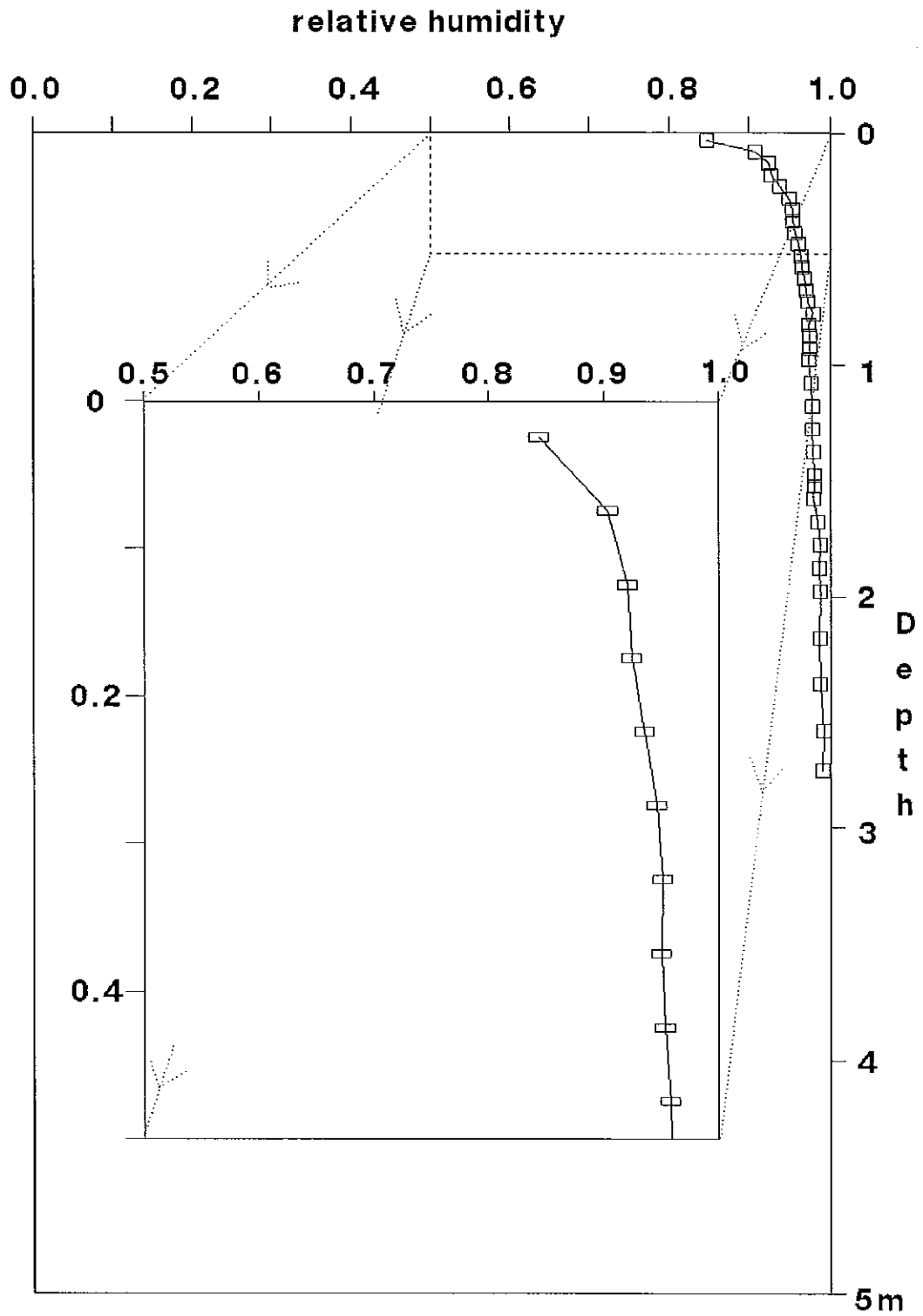


FIGURE 5.1.4 Calculated Relative Humidity Profile, Hole 18

# Hole 20 depth vs relative humidity

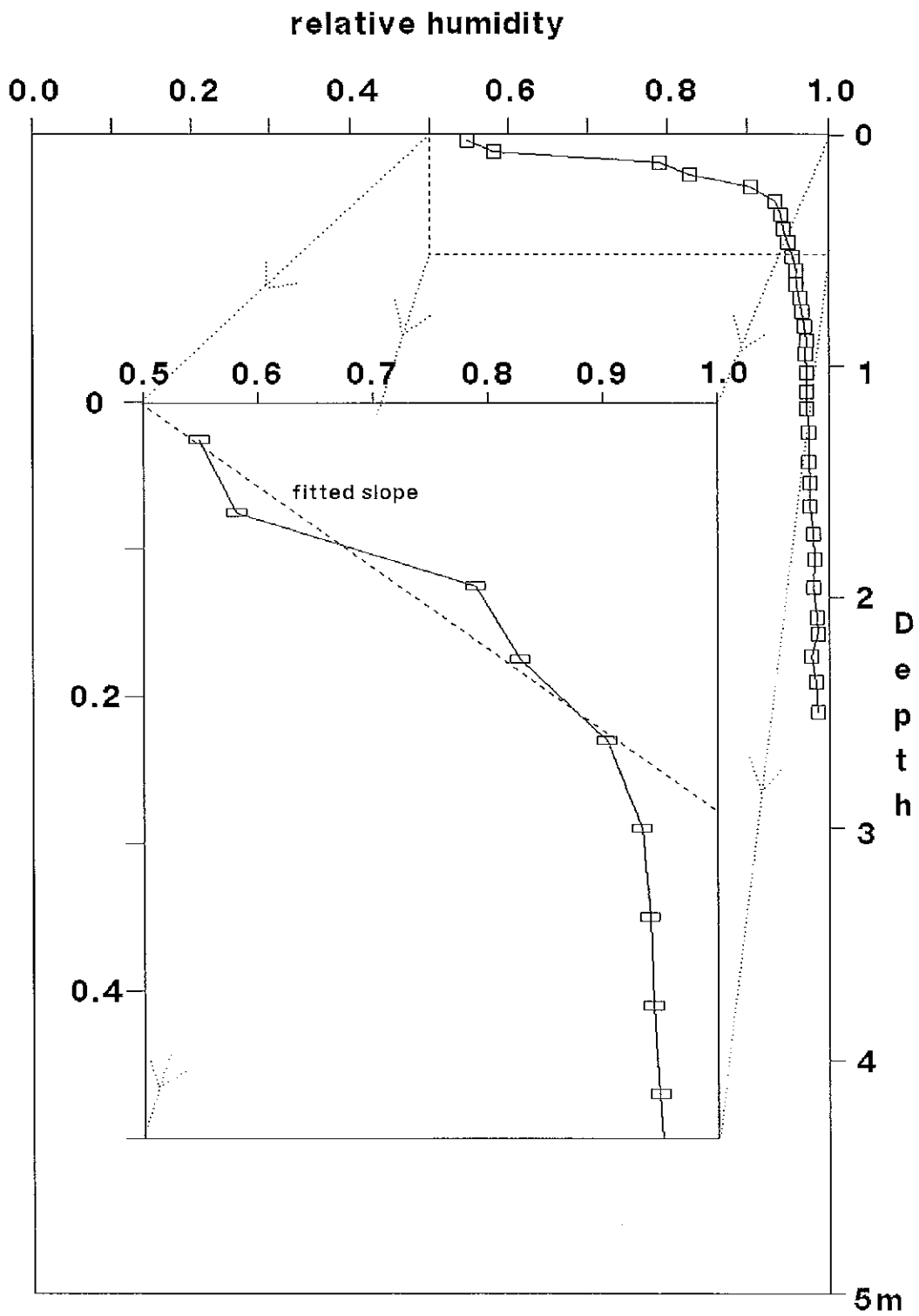


FIGURE 5.1.5 Calculated Relative Humidity Profile, Hole 20

### Hole 21 depth vs relative humidity

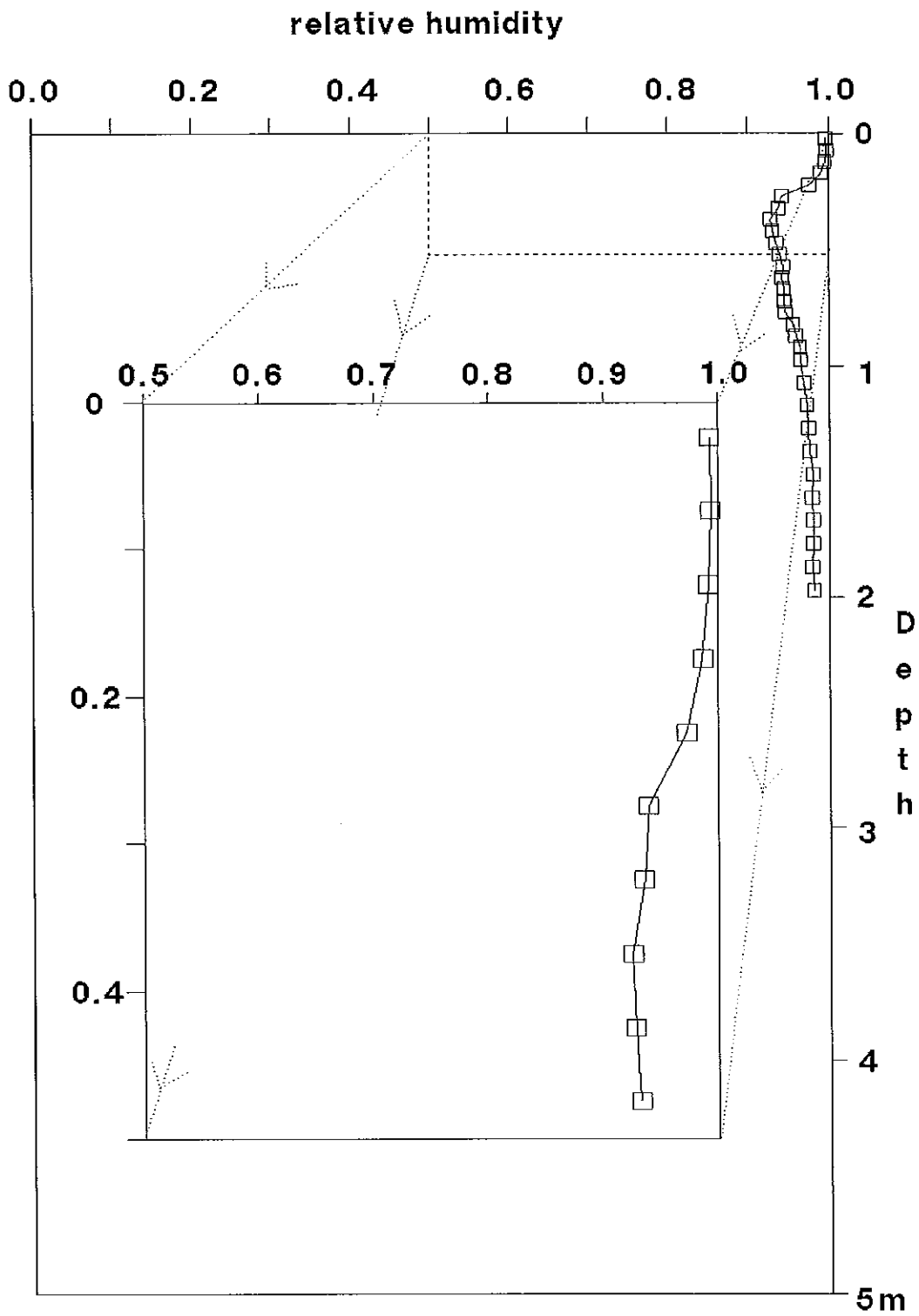


FIGURE 5.1.6 Calculated Relative Humidity Profile, Hole 21

TABLE 5.1.2

## Water Vapour Flux Estimates, Hamilton Hill Site

Hole	Slope $\text{m}^{-1}$	Flux estimate $\text{mm yr}^{-1}$
18 (top)	1.20	4.9
18 (.075-.225m)	0.20	0.8
20 (.025-.225m)	$1.9 \pm 0.4^*$	$7.6 \pm 1.2$

\* Slope and error from regression analysis

profile, so that there is the possibility of (minor) vapour movement even to that depth, here about 2.0 to 2.5 m.

The profile of hole 21 shows that due to the dilution of the soil solution by infiltrating rain and/or flood water, there is in fact a downward vapour gradient that would tend to redistribute water in the soil profile towards the salty zone. It should be remembered that the gradient into the atmosphere from the very top of the profile is still very great, so atmospheric vapour is not being added to the profile at this time. The high suctions and low relative humidities of the soil air at the surface in the other holes demonstrate the potential for some accession of atmospheric vapour into the soil profile when the outside relative humidity is high, such as occurs at night, particularly in the winter months.



### 5.1.5 ELECTROMAGNETIC CONDUCTIVITY SURVEY

The results of the electromagnetic conductivity survey taken along a 320 m transect south of hole 20 on 29-3-88 are shown in figure 5.1.7. Although an apparent conductivity is measured, the figures perhaps give some idea of the uniformity of the distribution of chloride beneath the ground surface, and hence the representativeness of the hole drilled.

The apparent conductivity drops going away from the site of hole 20, from  $420 \text{ mS m}^{-1}$  around the hole (within the radius that the holes 4 and 18 were drilled in), to about 200 in lower lying ground to the south. There were signs of water ponding in the lower conductivity areas, in contrast to the site of the holes which was chosen in an area free of such signs; however apparent conductivity rose at the location of a minor channel.

The reading of an EM induction meter depends on both the salinity and water content of the ground beneath, so that without proper calibration from drilled holes no quantitative interpretation may be made. The lower reading in slightly lower lying ground compared to the higher is probably due to lower salinity of the ground and/or soil water, or to a higher sand/lower water content. Likewise the high reading at the minor channel could be due to more salt or more water. No firm conclusions can be made regarding the relationship of EM reading to discharge at this site, only that the distribution of water and salt is not very uniform over the order of tens of metres. It is the similarity of evaporation estimates from the three holes at the site and nearby hole 18, where lithology, water and salt contents do vary, that gives confidence in the evaporation figures obtained at this site.

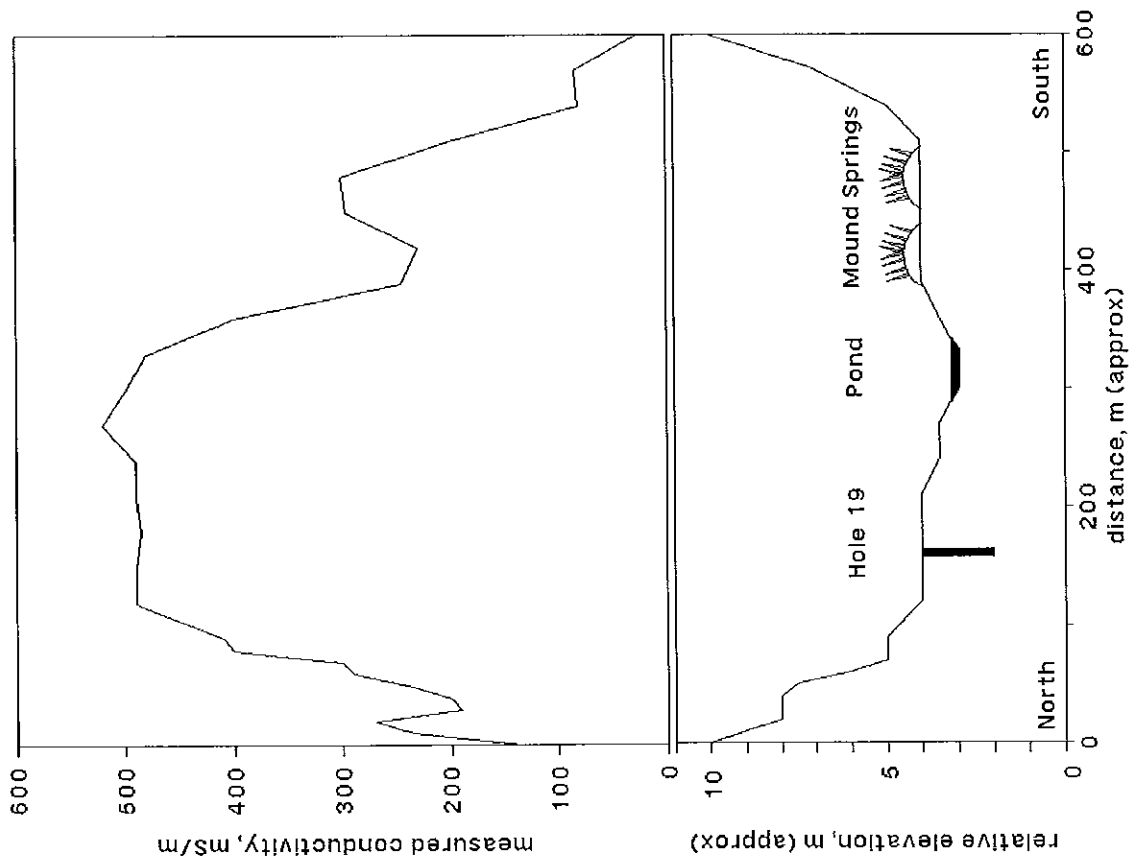


FIGURE 5.2.6 Electromagnetic conductivity survey, Hermit Hill

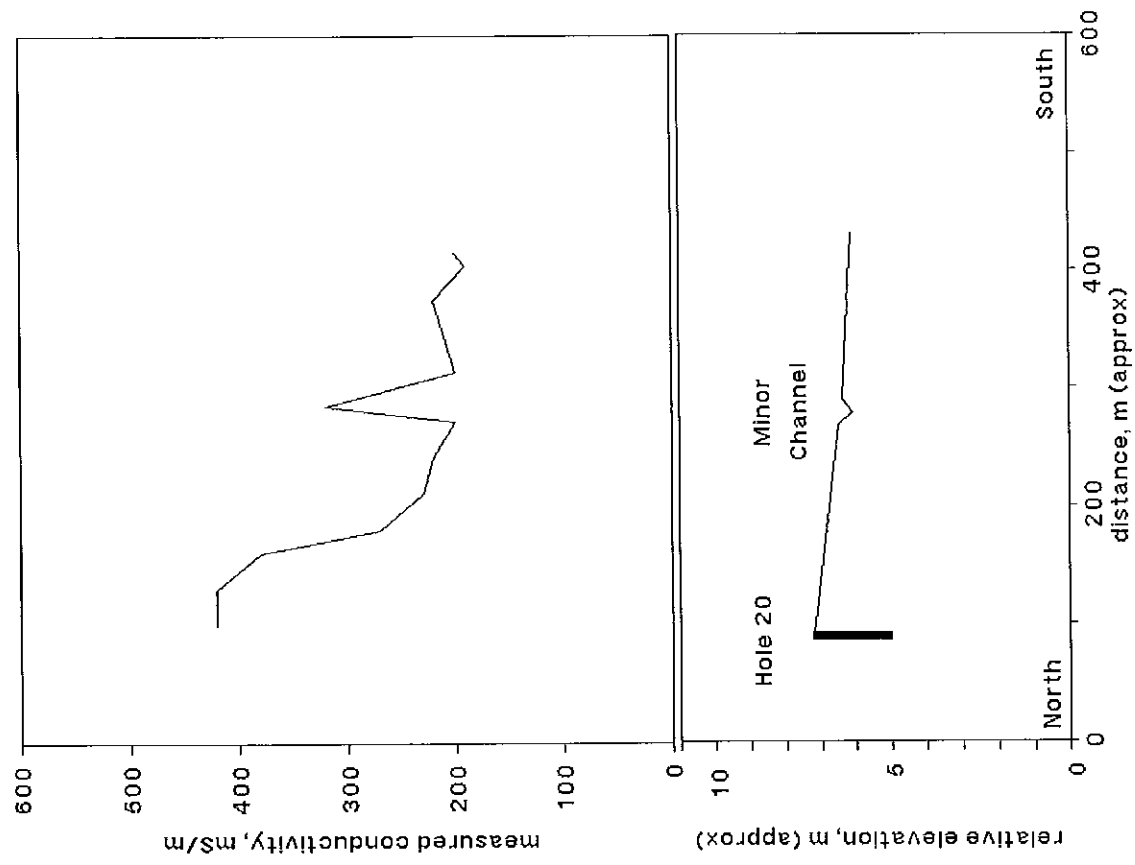


FIGURE 5.1.7 Electromagnetic conductivity survey, Hamilton Hill

## 5.2 HERMIT HILL: HOLES 1, 17, 19

### 5.2.1 NOTES ON TIME-SERIES

The Hermit Hill site is on a gravel bank, about 2m above the sandy base of Wergowerangerilinna Creek, on the north side of Hermit Hill. The bank is about 50 m wide, flanked to the north by low sand dunes, and the south by the creek. The holes were drilled in the centre of the bank within about 10m of each other. Unfortunately the site could not be accessed in April 1989, so the time series is not as extensive as the Hamilton Hill site.

The lithology of the holes is very similar, as noted in the descriptions and shown in the water content profiles (Fig. 5.2.1a.). The base of the alluvial sediments is well marked by the very damp, most weathered part of the Bulldog Shale beneath, the transition between about 0.6 and 0.8m. The chloride and deuterium profiles (Fig. 5.2.1b,c) are similar below about 0.7m (i.e. in the shale). Hole 1 (Sept. 1986) shows an evaporation profile that has been disrupted at the top by infiltration in the recent past, with evaporative concentration just noticeable in the top sample (0.0-0.05m) of chloride, and to about 0.15m with deuterium.

By July 1987, the peak of these solutes appears to have been displaced downwards; this is probably due to mixing of the pre-existing, heavy (and chloride rich) water with the lighter, fresher water that had infiltrated. Near the surface evaporation has increased the salt level to the precipitation of halite; the deuterium level is in fact lower than the previous year. This is assigned to exchange with atmospheric vapour during winter when evaporation rates are at their lowest, and average relative humidity at its highest. With the presence of halite at the surface, atmospheric vapour will condense onto the soil surface when the

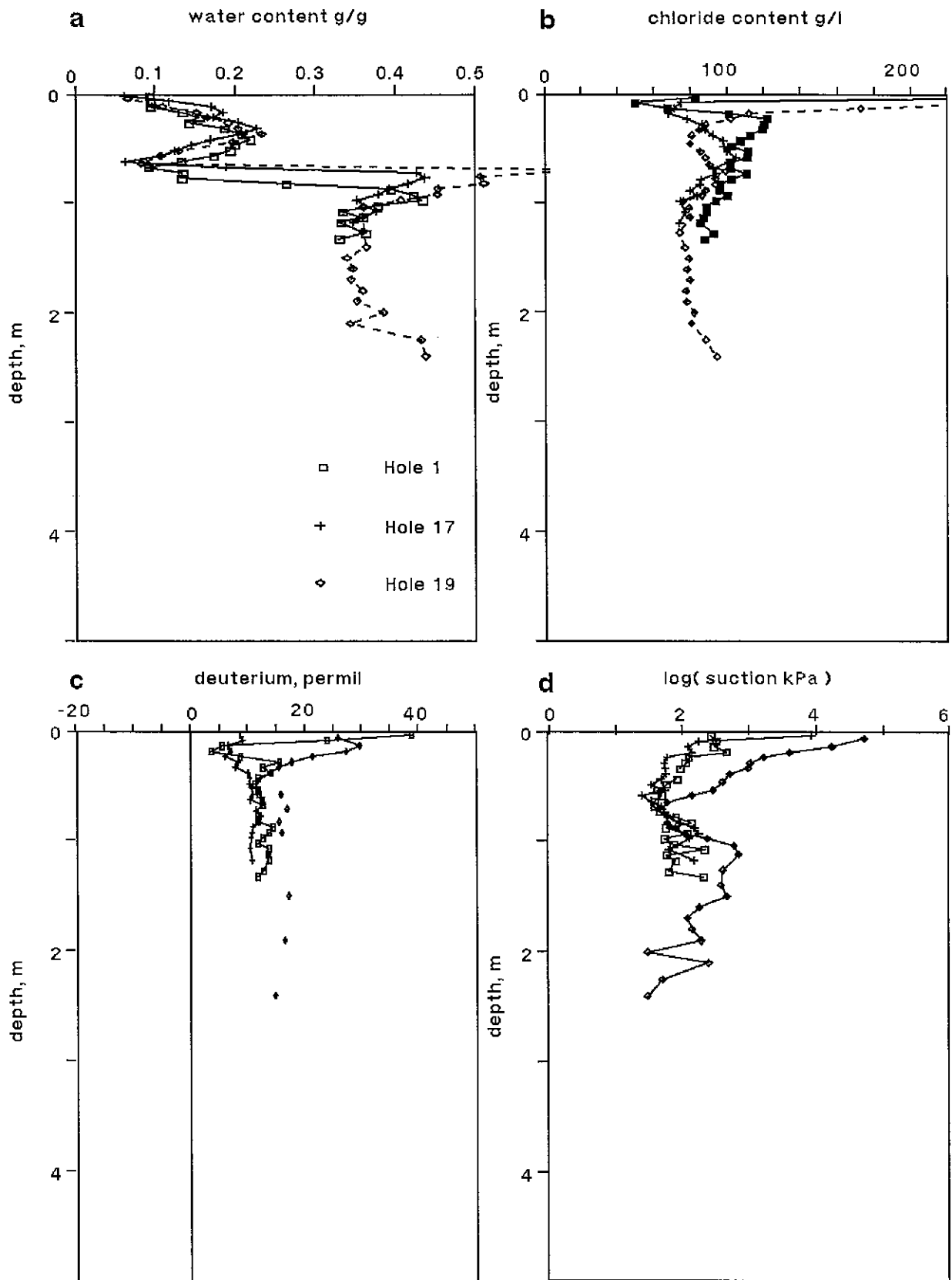


FIGURE 5.2.1 Profile Comparisons, Hermit Hill

relative humidity exceeds about 77%, which happens on some nights (winter frost and dew are known in the area, implying a relative humidity of 100% occurs at times). Any light rain, even if it infiltrates only a few millimetres, would also tend to lighten the isotopic signature of soil water near the surface, even if the nett water movement is one of evaporation, as is probably the case here.

At the end of the summer of 1987/8 further evaporation had lead to more halite deposition at the surface, and the chloride "minimum" has moved deeper into the profile as well.

The cumulative chloride profiles for these holes are all very similar and are not presented, providing no further information. The matric suction profiles in figure 5.2.1d provide further evidence of the progressive drying out of the top of the profile over the observation period. The scatter of the data in the shale is probably more due to the inaccuracy of the method than to real suction differences.

## 5.2.2 EVAPORATION ESTIMATE

The lower part of the chloride profile from hole 1 appears to be a remnant from a long period of evaporation without infiltration, and so an evaporation estimate is attempted from that data. The plot of  $\ln(c - c_{res})$  against depth is given in figure 5.2.2. The shallow reservoir case is that using the deepest chloride value of the profile: this is very close to the value obtained from the water table in the deeper hole 19. Using  $\theta_v \cong 0.48 \text{ m}^3 \text{ m}^{-3}$  and  $f_1 = 0.33$ , evaporation is estimated as below in table 5.2.1. The characteristic time is 800 years for the deep reservoir case.

TABLE 5.2.1

Evaporation Estimate, Hermit Hill Site, Hole 1

---

a. Deep Reservoir

$R^2$	Slope $m^{-1}$	Evaporation $mm\ yr^{-1}$
0.864	$-0.312 \pm 0.028$	$2.8 \pm 0.2$

---

b: Shallow Reservoir

$R^2$	Slope $m^{-1}$	E/D $m^{-1}$	Evaporation $mm\ yr^{-1}$
0.72	$-2.613 \pm 0.344$	-2.35	21

---

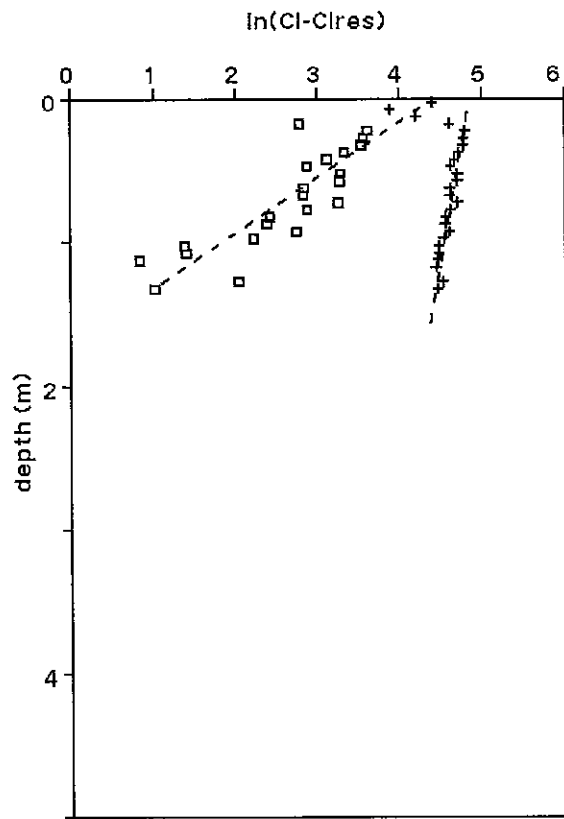


FIGURE 5.2.2 Hole 1 ln(Cl-C/res) vs depth plot

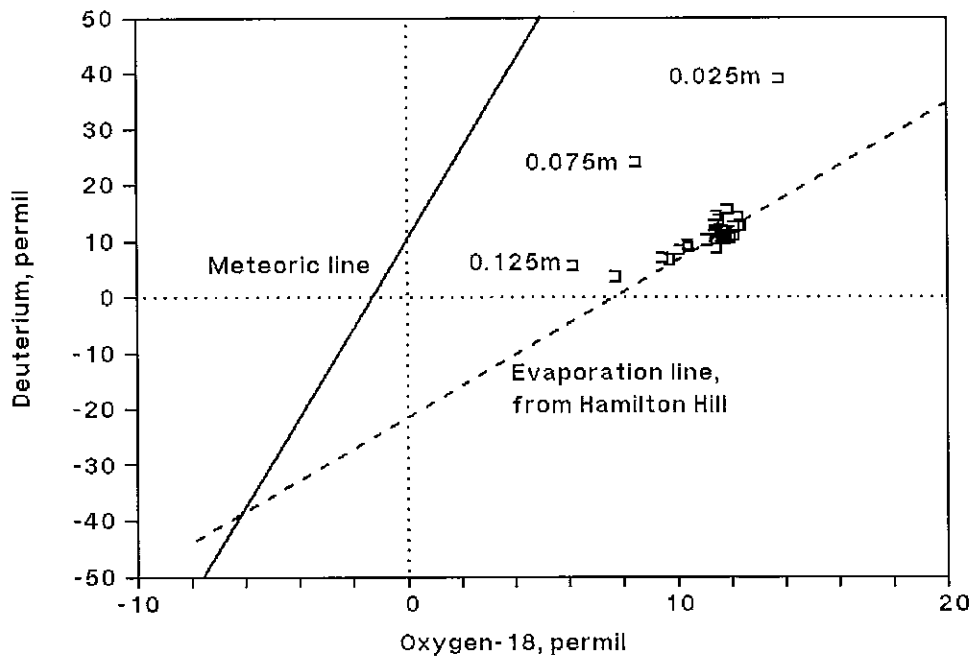


FIGURE 5.2.3 Hermit Hill Site Pore Waters, O-18 - D Plot

### 5.2.3 OXYGEN-18 - DEUTERIUM RELATIONSHIP

The data from holes 1 and 17 are plotted on figure 5.2.3, compared to the meteoric line. The data is not suitable for linear regression analysis, but the "evaporation line" from Hamilton Hill is included for comparison. Apart from the top three samples from hole 4, which are marked, the values are consistent with those obtained at Hamilton Hill. The top three values from hole 1 are thought to be affected by infiltration, and indeed lie somewhat closer to the meteoric line. As with the previous site, the low slope of the data (2.80) is consistent with evaporation through a layer of dry soil (slope of 2 to 5; Barnes & Allison, 1983, see section 2.1.2).

### 5.2.4 WATER VAPOUR FLUX ESTIMATES

Graphs of calculated relative humidity against depth for holes 17 and 19 are given in figures 5.2.4 and 5. The slopes are 3.6 and 2.3  $\text{m}^{-1}$  respectively, corresponding to fluxes of 15 and 10  $\text{mm yr}^{-1}$ . These are between the estimates from the chloride profile of hole 1, three and 21  $\text{mm yr}^{-1}$ , depending on the boundary condition chosen.

### 5.2.5 ELECTROMAGNETIC CONDUCTIVITY SURVEY

The results of the Hermit Hill EM survey of 29-3-89 are shown in figure 5.2.6. A view looking south along the transect is shown in Plate 5.1. The survey shows a plateau of high apparent conductivity, 490  $\text{mS m}^{-1}$ , on all of the bare, flat bank that holes 1, 17 and 19 are drilled on. Conductivity drops off to the north, where there are lightly vegetated dunes a few meters above the bank. The lower values probably reflect both a deeper water table relative to the surface, and less salt



### Hole 17 depth vs relative humidity

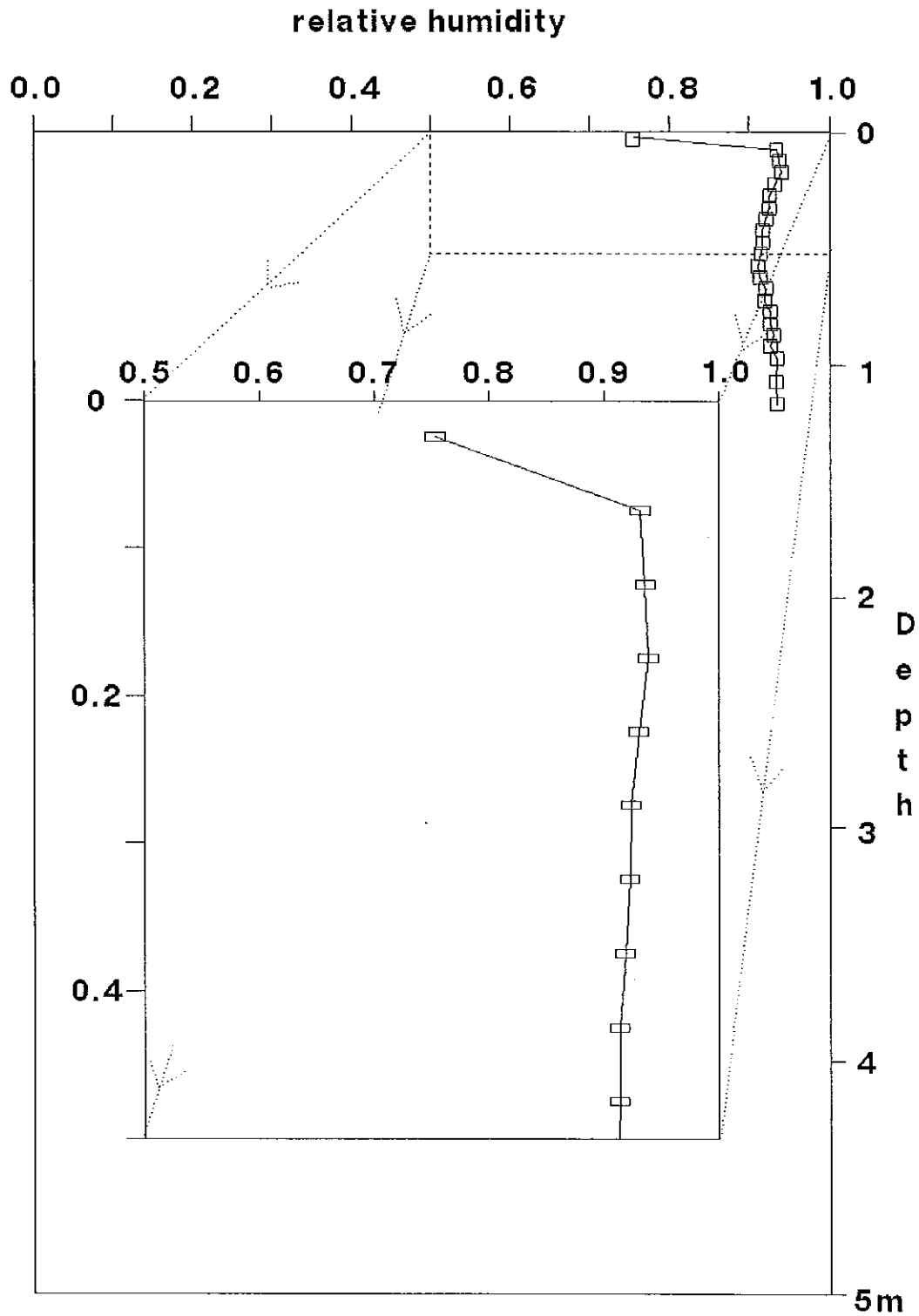


FIGURE 5.2.4 Calculated Relative Humidity Profile, Hole 17

### Hole 19 depth vs relative humidity

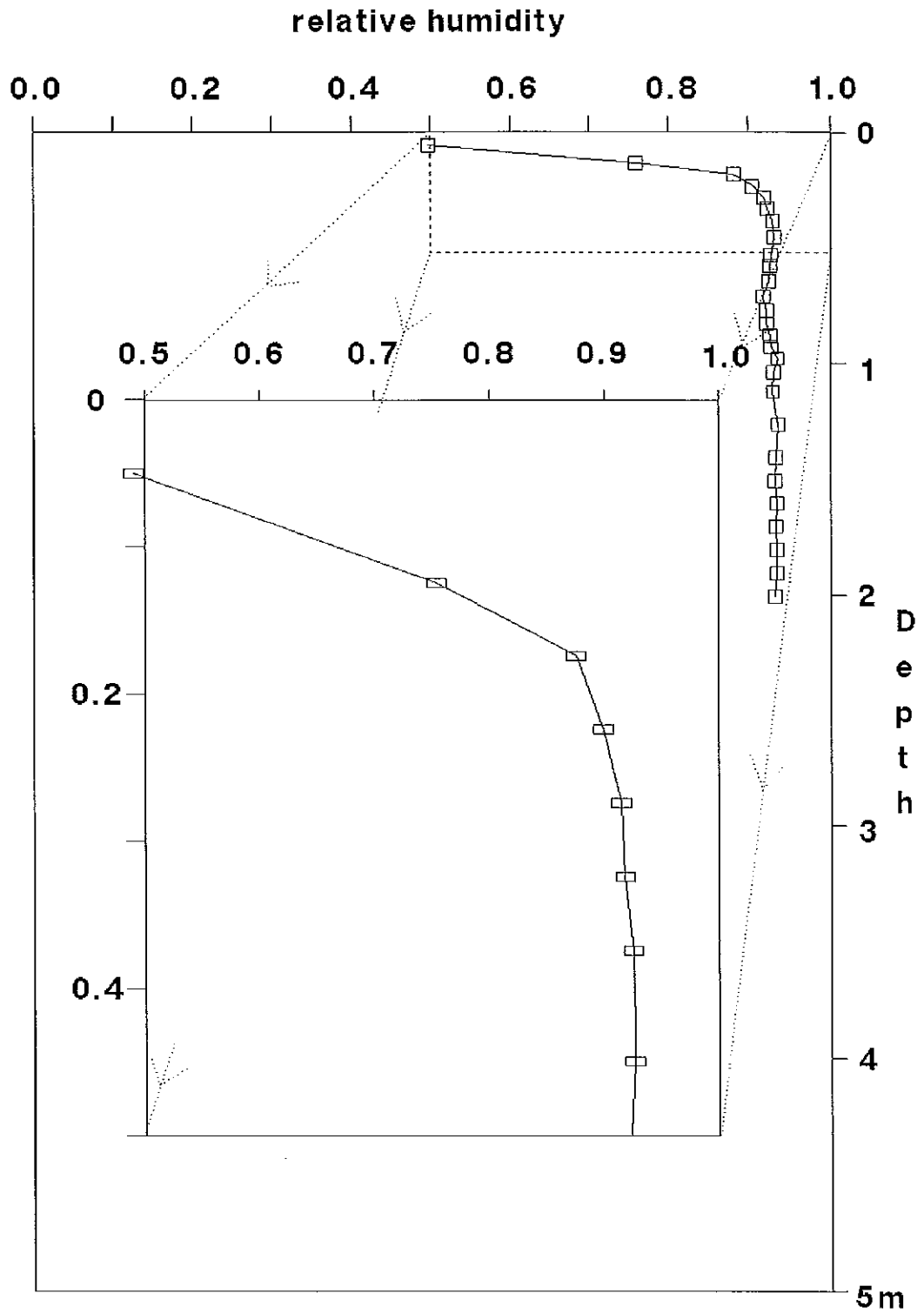


FIGURE 5.2.5 Calculated Relative Humidity Profile, Hole 19

in the soil, as evidenced by the vegetation. There is a general drop in conductivity towards the mound springs; this is probably due to the freshening effect of the spring waters on the shallow groundwater, the ground being saturated with water around the springs and shallow pool in the creek bed. The values become very low south of the springs on the flanks of Hermit Hill itself. The Hill consists of Pre-Cambrian rock and is not part of the Great Artesian Basin, so no pressure aquifer exists beneath the surface to force upward movement of water. There is probably a small net recharge to the water table beneath the fractured rock of the hill, and enough relief so that water movement is downward and sideways into the edge of the spring areas below. Hence there is no build up to the high concentration of salt in the soil profile as exists on the gravel bank, and to a lesser extent (probably) beneath the dunes on the other side of the creek. The conductivity shows a good inverse relationship to topography, modified a little by the presence of the springs, and again cannot be directly linked to evaporation rate.



PLATE 5.1 View looking south along the electromagnetic conductivity survey transect line past the site of holes 1, 17 and 19 (at vehicle) and some mound springs to Hermit Hill. March 1988

### 5.3 SITE GAB 6: HOLES 10, 23, 24

#### 5.3.1 NOTES ON SERIES

Holes in this series are near Olympic Dam Project's production bore GAB 6, drilled on gibber plain about 4 km south of the bore. A hole was attempted in September 1986 by hand auger, and abandoned due to gypcrete a few tens of centimetres down (no data), the rig was successfully used in October 1986, and two holes hand augered in April 1989 using a narrower auger. The last two holes were sited twenty-five metres apart on the same patch of bare gibber, hole 23 on a slight rise, and hole 24 in a slight depression where there were signs of ponding of water in the recent past (see Plate 4.2 in the previous chapter). They were intended to check for infiltration following the heavy March 1989 rains.

The lithology of holes 23 and 24 are quite similar, as seen by their gypsum profiles (Fig. 5.3.1b). Hole 24 was noticeably wetter than hole 23 (Fig. 5.3.1a), but in this case that does not appear to reflect higher clay content, but rather greater infiltration of water after the rain event. Hole 10 is within about 200 m of the same site, and has a much thicker gypsum-free layer below the surface, down to about 1.5 m compared to about 0.4 m. There are more small layers of sandier and clayier material in hole 10, as revealed by the water content and bulk soil chloride profiles (Figs. 5.3.1 a & g). These differences may well affect the other characteristics of the profiles so that comparisons of 23 and 24 to hole 10 are approximate only.

Hole 10 has halite near the surface, but neither holes 23 nor 24 have as high soil solution concentrations (Fig. 5.3.1c). Hole 23 shows a similar shaped profile to that of 10, except near the surface where it appears to have been affected by infiltration. The concentration in hole

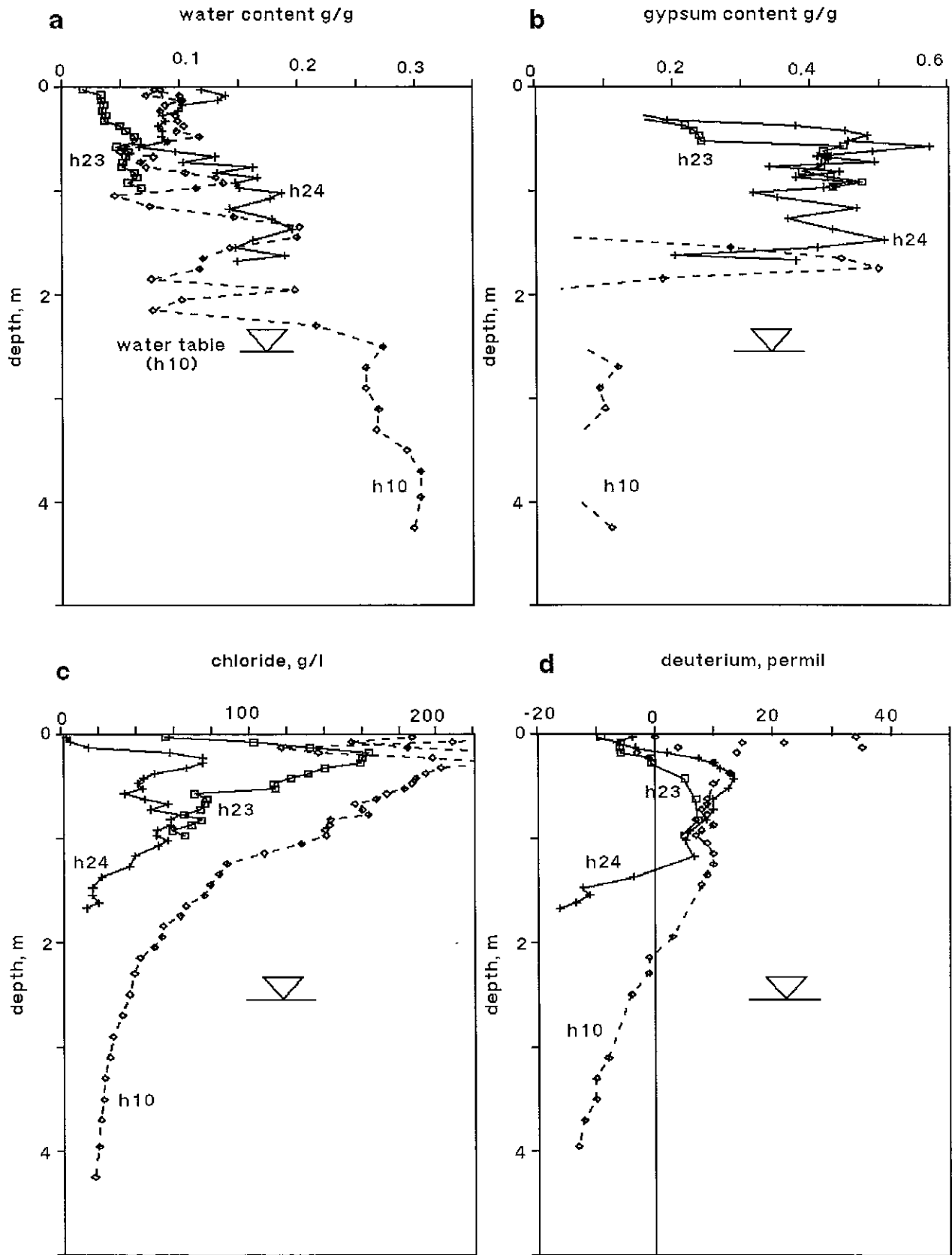


FIGURE 5.3.1 Profile Comparisons, GAB 6 Site

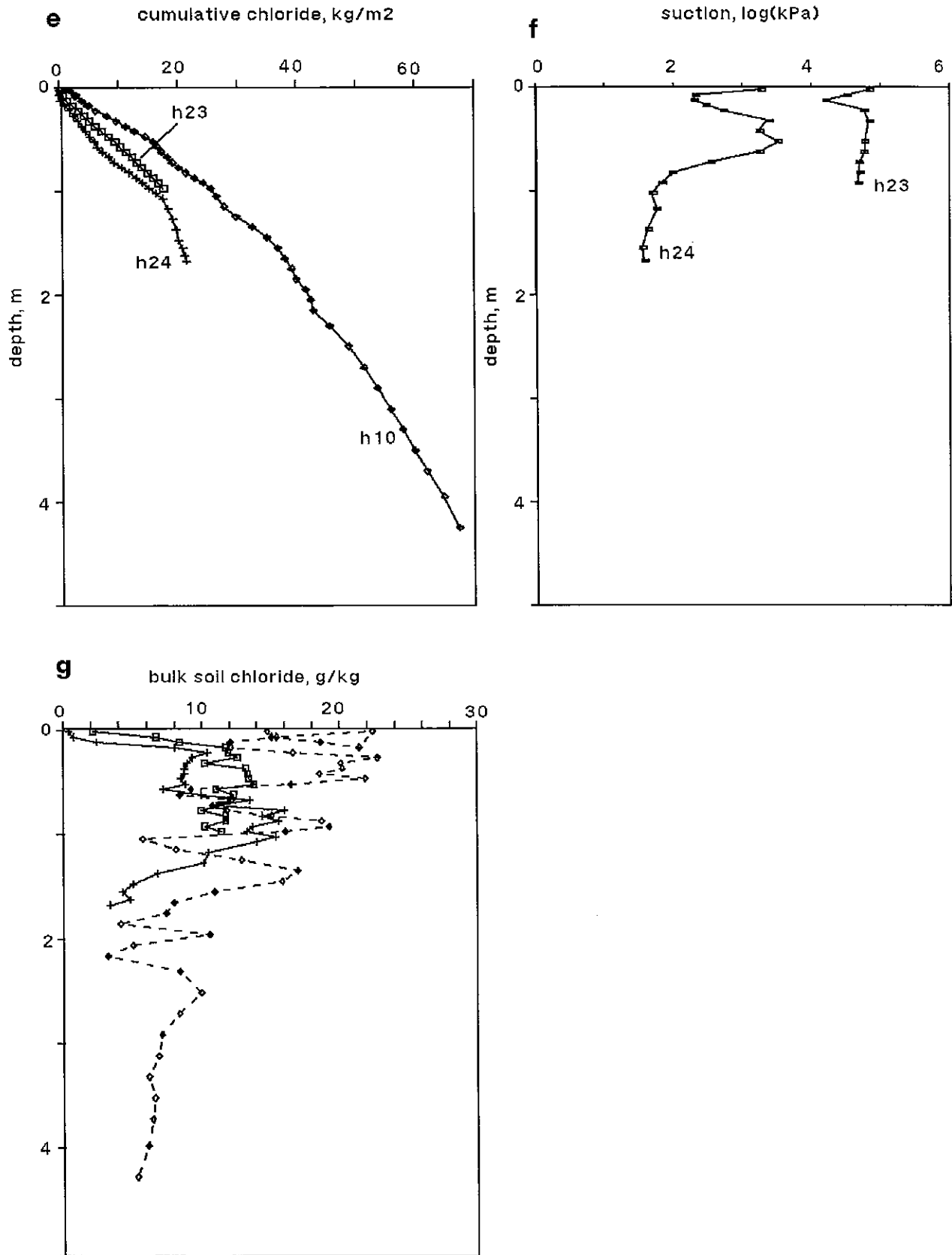


FIGURE 5.3.1 (Continued) Profile Comparisons, GAB6 Site

24 is lower again, except at about 0.8 to 1.0 m where they are very similar, and the near-surface flushing is more pronounced. The flushing is confirmed by the bulk soil chloride concentrations, which show the total amount of chloride has decreased, and that the decreased soil solution concentration is not just due to higher water content.

The deuterium values at the surface are much more enriched in hole 10, but the values from about 0.3 m to 1.2 m are quite similar (Fig. 5.3.1d). Below this, hole 10 data shows a slow, exponential decline with depth, but hole 24 drops off very quickly. The suction profiles of holes 23 and 24 (Fig. 5.3.1e) suggest how the chloride and deuterium contrasts between those holes came about. Infiltrating water moved fairly quickly through large pores of the upper part of the gypseous part of the profiles, where the structure of the soil is fairly open, because of the disruptive, in situ growth of the gypsum crystals. Some chloride was leached, but the water in small pores was left behind, retaining the original isotopic composition and the remaining chloride. Because the passage of the infiltrating water was swift, only minor exchange with the fine-pore water occurred. Deeper in the profile, the gypsum content generally drops off, and the profile becomes clayier, resulting in lower hydraulic conductivity and slowing down of the infiltrating water. Hence the soil at this depth wet up (low suction), and the influence of the fresh water on the stable isotope and chloride concentration of the soil water is strong. This "preferred pathway" flow is in contrast to the possible "piston flow" inferred from hole 21.

Because of time constraints, hole 24 could not be deepened to the water table, at about 2.4 m in hole 10. It seems reasonable that a portion of the infiltrating water did reach the water table at this location and constitute recharge, as was inferred for the area because of the saline base flow in the creeks (section 4.2.2). Infiltration at

nearby hole 23, on a slight rise with no sign of ponding, shows evidence of very shallow infiltration only, probably associated with no recharge to the shallow aquifer. Another hole on gibber plain drilled the same day some kilometres away (hole 22) shows the same minor, shallow infiltration at another site where there was no evidence of ponding. Recharge to the shallow aquifer was apparently significant overall, but very patchy on the small scale. Profiles of solutes were virtually unaffected beneath areas of no ponding, so that the deep profiles obtained from such sites where also horizontal movement of water in the shallow aquifer is not important do reflect very long-term processes, making the use of steady-state theory quite appropriate.

### 5.3.2 EVAPORATION ESTIMATES

The data of hole 10 is the most appropriate of all the gibber plain holes for the application of the convection-diffusion theory to estimate diffusion, as the water table appears to have no influence on the profiles except to increase the water content. Plots of  $\ln(c-c_{res})$  against depth are shown in figure 5.3.2, and evaporation estimates laid out in table 5.3.1.

There is no well defined peak in the deuterium profile, and the samples near the surface are quite scattered. This is probably due to shallow infiltration of rain water followed by evaporation, and also that data from the shallow hole 10A (dug by spade to 0.20m) is plotted with that from the deep hole. If only data from below about 1.2 m was used, the slope and evaporation estimate would only be a little greater. The less prominent peak is probably due to the importance of vapour phase movement of water to quite significant depths in the profile; the presence of high concentrations of chloride means a significant vapour



concentration gradient exists down to a metre or two (c.f. vapour flux calculations), so that there is an evaporation "zone" rather than "front", as apparent in work such as at Lake Frome (Barnes & Allison, 1985) and elsewhere, and to a lesser extent in the flood plain holes of this project.

In the deeper part of the profile where vapour movement is indeed small, chloride and deuterium give similar estimates of evaporation. In the upper part, chloride is only transported in the liquid phase, so that the water movement (evaporation) estimate is smaller. The deuterium calculation uses an impedance factor that allows for vapour movement (section 2.2.4) and shows the same rate throughout the profile. Vapour movement appears to be at least as important as liquid movement in the upper part of the profile (0.3 to 2.2m, or virtually to the water table).

TABLE 5.3.1

Evaporation Estimate, GAB 6 Site, Hole 10

Solute	$R^2$	$\theta_v$ $m^3 m^{-3}$	$f_1$	Slope $m^{-1}$	Evaporation $mm yr^{-1}$
Chloride (upper)	0.989	0.16	0.078	$-0.891 \pm 0.019$	$0.56 \pm 0.01$
Chloride (lower)	0.973	0.48	0.33	$-0.431 \pm 0.024$	$3.5 \pm 0.2$
Deuterium	0.948	0.32	0.50	$-0.144 \pm 0.007$	$1.6 \pm 0.1$

### 5.3.3 OXYGEN-18 - DEUTERIUM RELATIONSHIP

The stable isotope relationship of pore waters from hole 10 is given in figure 5.3.3. Excluding three points from near the surface, the data gives a good fit to an "evaporation line",

$$\delta D = 2.31 \delta^{18}O - 21.7 \quad R^2 = 0.94 \quad (5.2)$$

with a standard error of slope of 0.16. The slope of the line is a little less than the 2.80 of the Hamilton Hill site, but still within the 2 to 5 reported by Barnes and Allison (1983) as typical of evaporation through a dry soil.

### 5.3.4 RELATIVE HUMIDITY PROFILE

The calculated relative humidity profile of hole 24 is given in figure 5.3.4. As with hole 21, it shows the potential for vapour movement redistribution of water within the soil profile, with a fairly strong gradient from the water table to the high-chloride zone of about  $0.062 \text{ m}^{-1}$ . Assuming  $p = 0.1$  and  $f_g = 0.6$ , this implies a flux of  $0.06 \text{ mm yr}^{-1}$ , or about 3% of the total flux estimated at hole 10.

## 5.4 OTHER GIBBER PLAIN SITES

### 5.4.1 EVAPORATION AND INFILTRATION ESTIMATES

Evaporation estimates may be attempted at several other gibber plain sites sampled during the project. Plots of  $\ln(c - c_{res})$  against depth are given in figures 5.4.1 to 5 for relevant holes. Calculations are presented in table 5.4.1, and discussed individually.

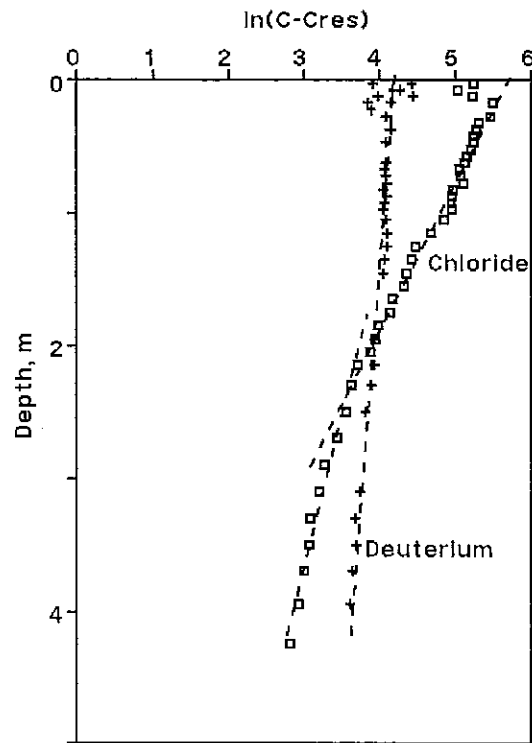


FIGURE 5.3.2 Hole 10,  $\ln(C-Cres)$  vs Depth Plot

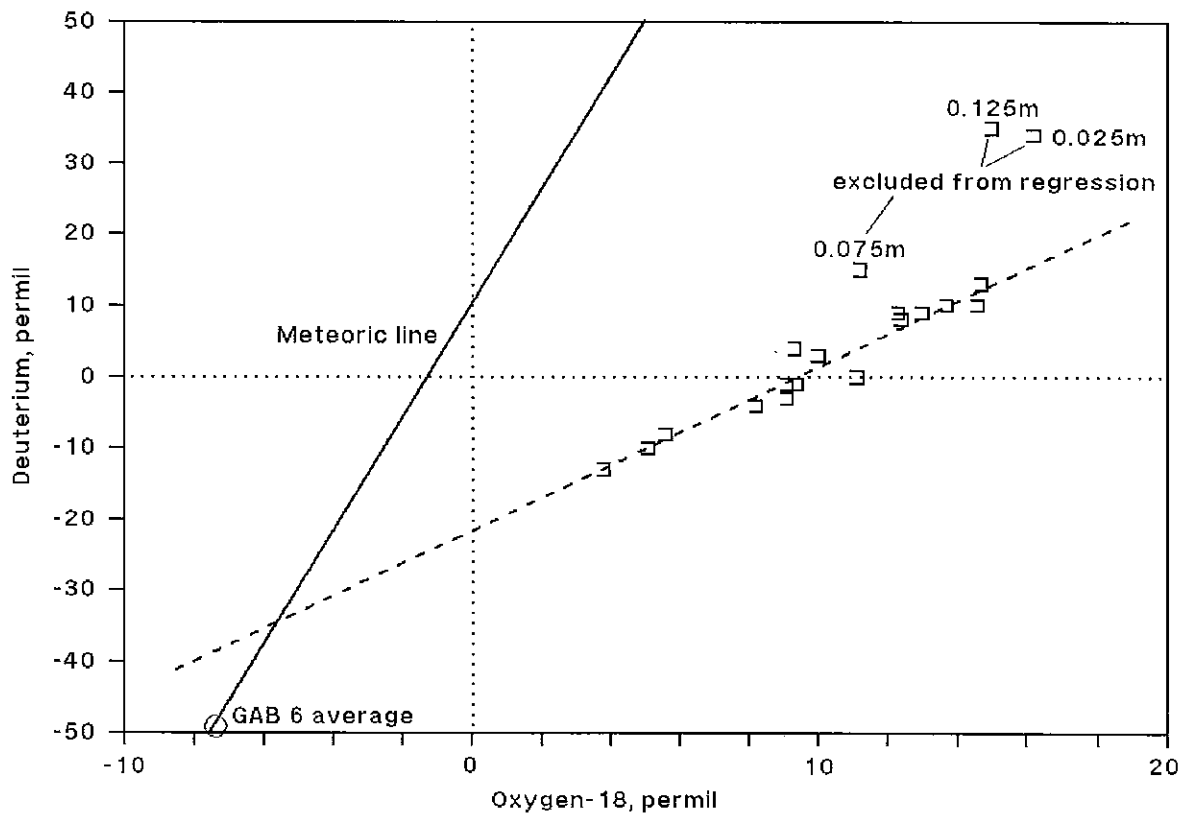


FIGURE 5.3.3 Hole 10 Pore Water O-18 - D Plot

### Hole 24 depth vs relative humidity

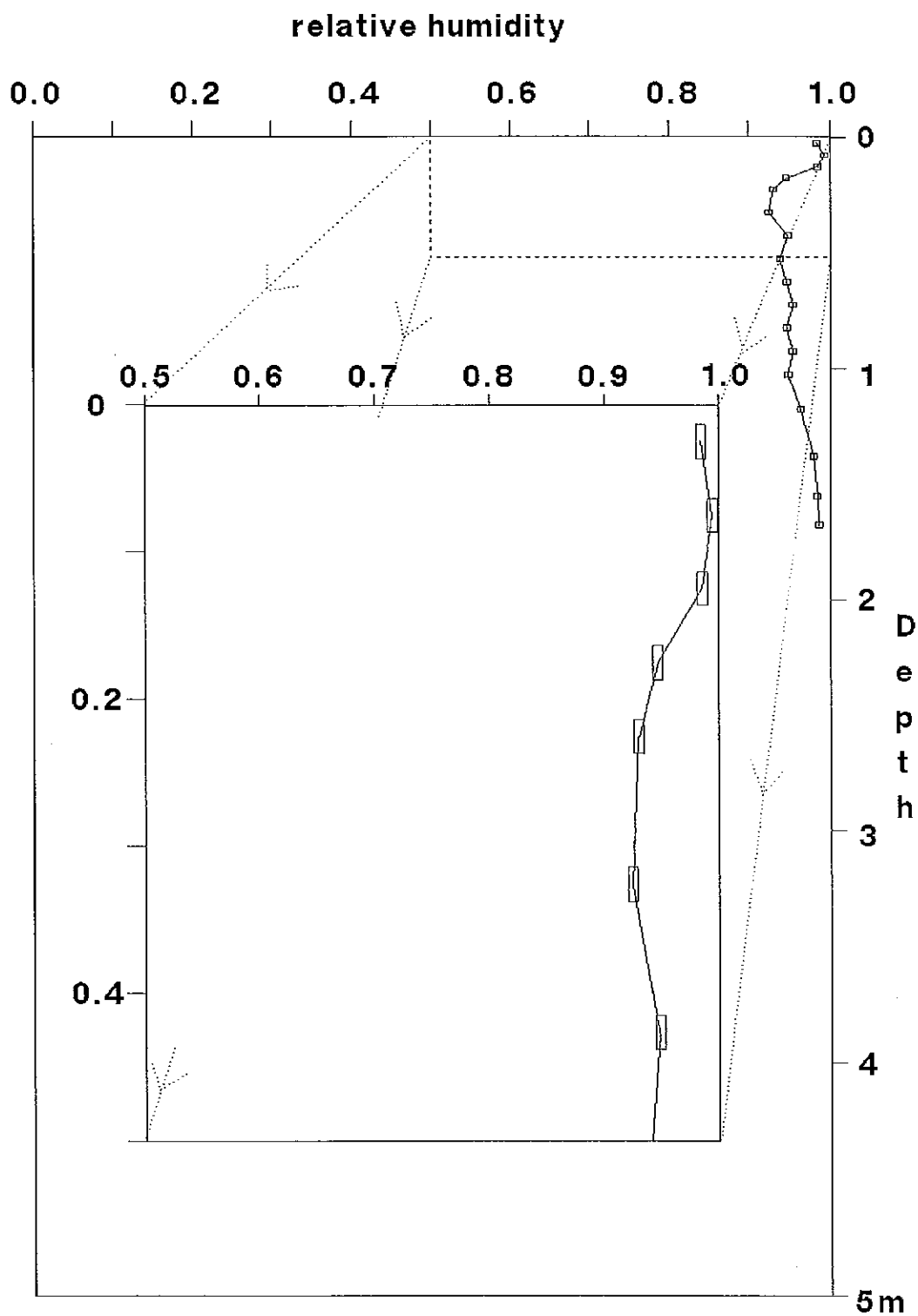


FIGURE 5.3.4 Calculated Relative Humidity Profile, Hole 24

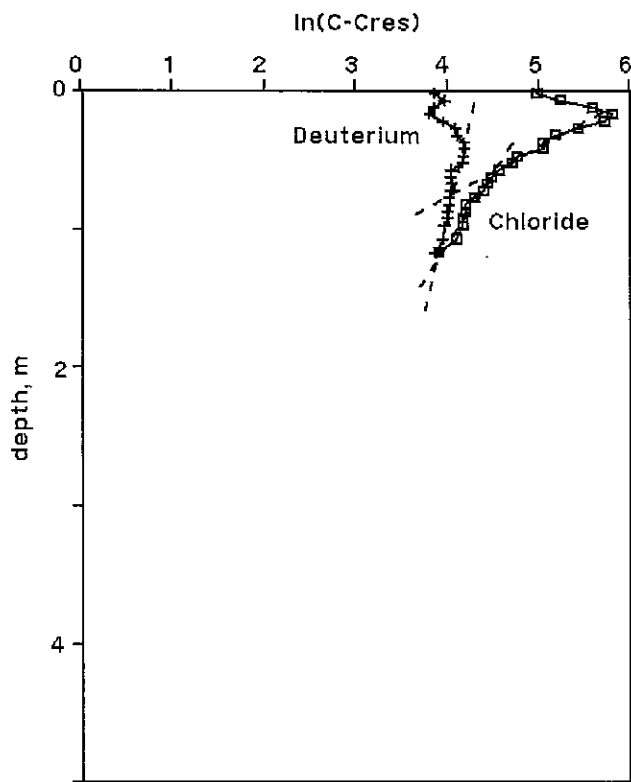


FIGURE 5.4.1 Hole 3, In(C-Cres) vs depth

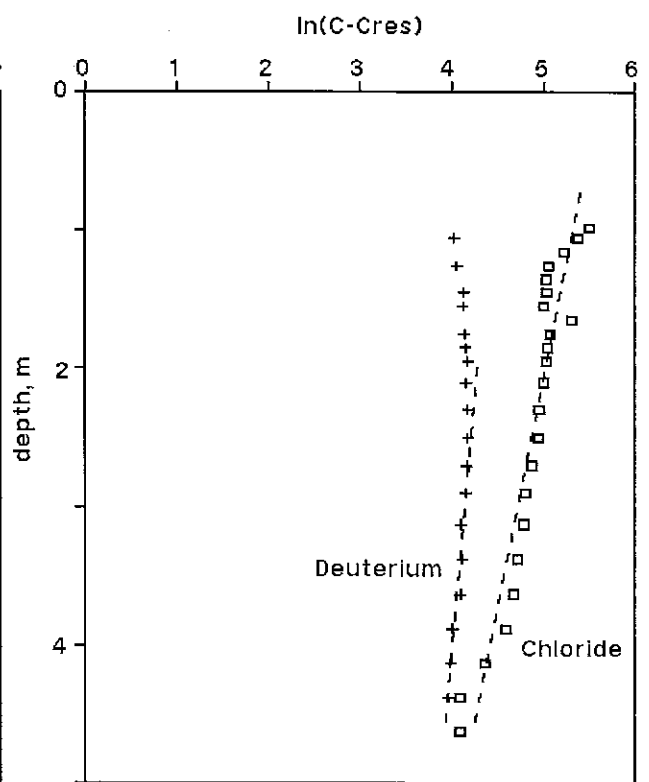


FIGURE 5.4.2 Hole 11, In(C-Cres) vs depth

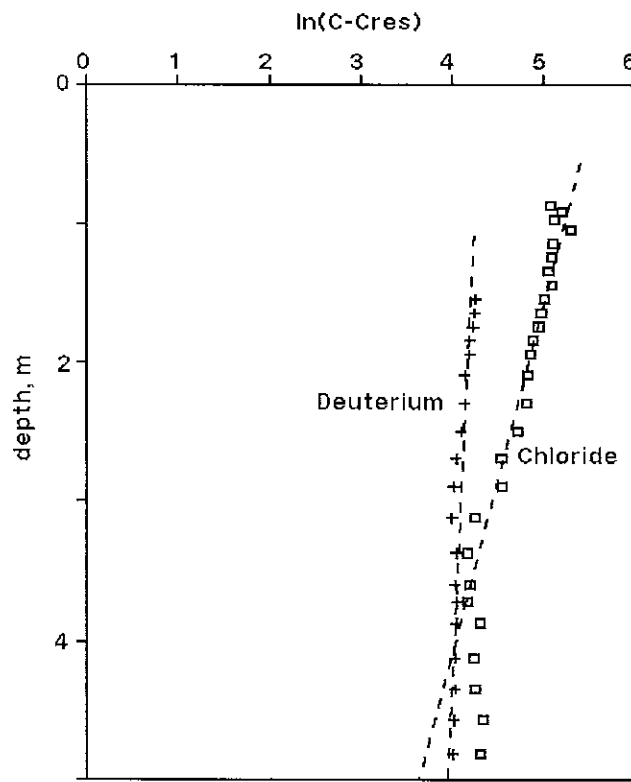


FIGURE 5.4.3 Hole 13, In(C-Cres) vs depth

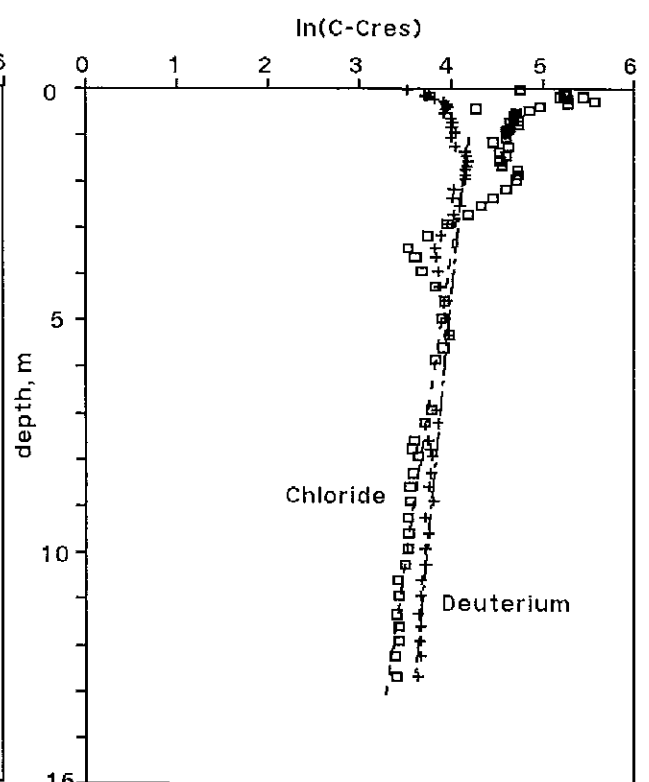


FIGURE 5.4.4 Hole 14, In(C-Cres) vs depth

TABLE 5.4.1

## Evaporation Estimates, Other Gibber Plain Sites

Hole	Solute	$R^2$	$\theta_v$ $m^3 m^{-3}$	$f_1$	Slope $m^{-1}$	Evaporation $mm yr^{-1}$
3	Cl (shallow)	0.964	0.16	0.078	$-2.742 \pm 0.238$	$1.7 \pm 0.2$
3	Cl (deep)	0.952	0.35	0.23	$-0.990 \pm 0.074$	$4.0 \pm 0.3$
3	$\delta D$	0.886	0.32	0.50	$-0.366 \pm 0.036$	$4.1 \pm 0.4$
11	Cl	0.896	0.29	0.18	$-0.298 \pm 0.021$	$0.8 \pm 0.1$
11	$\delta D$ (deep)	0.918	0.40	0.50	$-0.128 \pm 0.017$	$1.8 \pm 0.2$
13	Cl (middle)	0.940	0.32	0.21	$-0.397 \pm 0.029$	$1.3 \pm 0.1$
13	$\delta D$ (deep)	0.759	0.46	0.50	$-0.070 \pm 0.010$	$1.1 \pm 0.2$
14	Cl (deep)	0.914	0.40	0.27	$-0.074 \pm 0.005$	$0.40 \pm 0.03$
14	$\delta D$	0.861	0.35	0.50	$-0.042 \pm 0.003$	$0.51 \pm 0.03$
16B	Cl (shallow)	0.965	0.26	0.155	$-0.358 \pm 0.024$	$0.73 \pm 0.05$
16B	Cl (deep)	0.989	0.40	0.27	$-0.110 \pm 0.003$	$0.60 \pm 0.02$
16B	$\delta D$ (deep)	0.960	0.34	0.50	$-0.076 \pm 0.004$	$0.90 \pm 0.05$

Hole 3 near Fred Springs shows the same pattern as hole 10, on a smaller scale. Vapour transport means the estimate from chloride nearer the surface is about half that estimated from deeper chloride and by deuterium, of  $4 \text{ mm yr}^{-1}$ . The water table is quite close to the surface, about 1m judging by the water content profile, and the characteristic times of the profiles are short by local standards, from 210 to 670 years. An estimate of evaporation rate from the depth of the deuterium peak is  $3.2 \text{ mm yr}^{-1}$ , in good agreement with the other estimates.

Hole 11 has a very broad deuterium peak, associated with very high chloride content. An evaporation estimate from the bottom of the deuterium profile seems reasonable, and is about double the chloride estimate. The latter uses data from higher up the profile as well, and so probably does not allow for vapour movement. The chloride data is more extensive, the preferred estimate for the hole is taken as  $1.5 \text{ mm yr}^{-1}$ . The characteristic times are 4200 and 4400 years respectively, intermediate for the gibber plain sites.

Chloride and deuterium data for hole 13 give very similar results of  $1.3$  and  $1.1 \text{ mm yr}^{-1}$ , from the upper and lower parts of the profile respectively. The characteristic times are quite different, 1900 years for chloride, and 13 000 years for deuterium. Although there is much more halite near the surface than with hole 11, the concentrations drop off more quickly with depth, so that vapour movement is probably important to a lesser depth.

Hole 14 has a pronounced kink in its profiles at about 4 m, near the inferred water table. Chloride data has been interpreted only below this kink, deuterium above and below. The estimates are very similar, at  $0.4$  and  $0.5 \text{ mm yr}^{-1}$ , and characteristic times very long, 34 000 and 46 000 years.

Hole 16B has a smaller kink at the water table to hole 14, and the

chloride data has been interpreted above and below the kink, and those points excluded from the deuterium regression. All three estimates are similar, from 0.6 to 0.9 mm yr<sup>-1</sup>, and the characteristic time of the upper part of the chloride profile 3800 years, and the lower profiles 15,000 years. The deuterium peak is more evident than the other gibber holes except hole 3, and taking the peak to be at 0.25 m gives an evaporation rate of 0.7 mm yr<sup>-1</sup>, giving further confidence to the estimates.

Holes 5, 6 and 7 show the effects of shallow infiltration of the previous winters rainfall into salty soils. From the displacement of the chloride peak, infiltration is estimated from cumulative water to that depth, table 5.4.2.

TABLE 5.4.2

Infiltration Estimates, Holes 5, 6 and 7

Hole	Infiltration depth (m)	Infiltration (mm)
5	0.30	26
6	0.20	21
7	0.25	70

The estimated infiltrations are significant relative to the annual average rainfall of the district, but are unlikely to provide much recharge, if any, as the water table is tens of metres deep at these sites, and the infiltrated water would be lost to evaporation, probably within a few months.



#### 5.4.2 OXYGEN-18 - DEUTERIUM RELATIONSHIPS

Data from holes 2 and 3 are plotted on figure 5.4.6. The regression lines are similar to those from other holes,

$$\text{hole 2: } \delta D = 3.12 \delta^{18}O - 24.0 \quad R^2 = 0.979, \text{ and} \quad (5.3)$$

$$\text{hole 3: } \delta D = 2.01 \delta^{18}O - 19.1 \quad R^2 = 0.777, \quad (5.4)$$

with standard errors of slopes of 0.20 and 0.30. The evaporation line from hole 2 data crosses the meteoric line very close to the average value of local deep groundwater, although the profile is not suitable for a convection-diffusion calculation. The line for hole 3 crosses the meteoric line above the local groundwater value as do the lines for holes previously calculated.

The data from hole 11 was quite scattered (Fig. 5.4.7), with a best fit line of

$$\delta D = 3.57 \delta^{18}O - 37.6 \quad R^2 = 0.663,$$

and standard error of the slope of 0.51. The best fit line cuts the meteoric line below the average groundwater: an alternative fit passing through the groundwater value is shown, and is not inconsistent with the data, so the "best fit" cut is not taken as an indication of different behaviour to the other holes.

#### 5.5 INTERPRETATION OF STABLE ISOTOPE RESULTS FOR GYPSUM WATER

Most of the gypsum waters were analysed for deuterium only, and tend to be depleted relative to the soil water at the same depth by about 40%

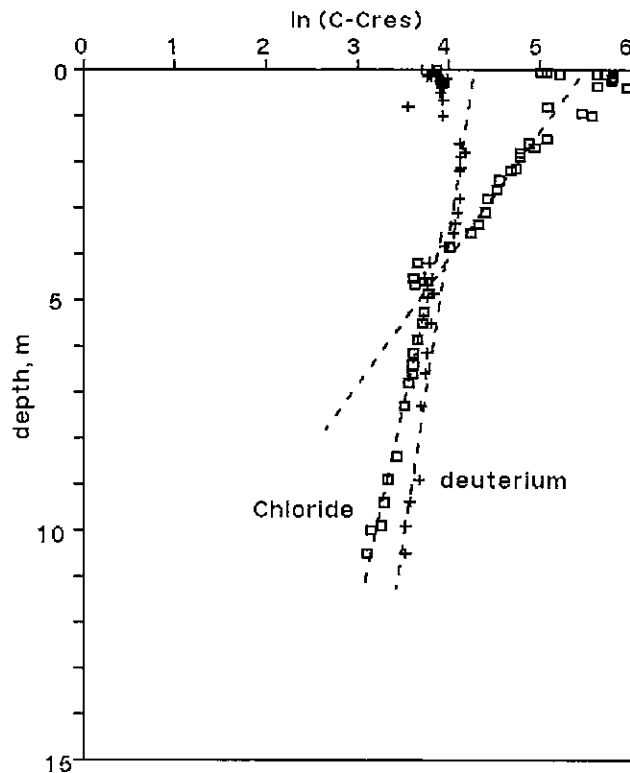


FIGURE 5.4.5 Hole 16 In(C-Cres) vs Depth Plot

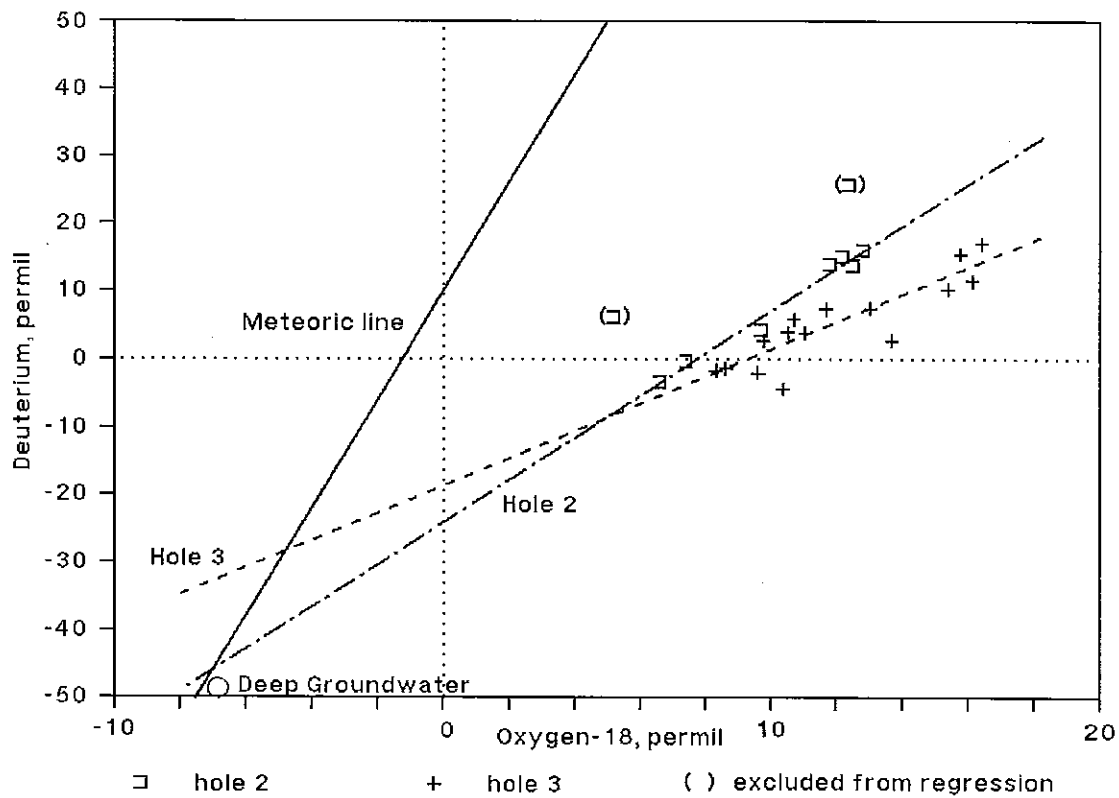


FIGURE 5.4.6 Holes 2 and 3 Pore Waters O-18 - D Plot

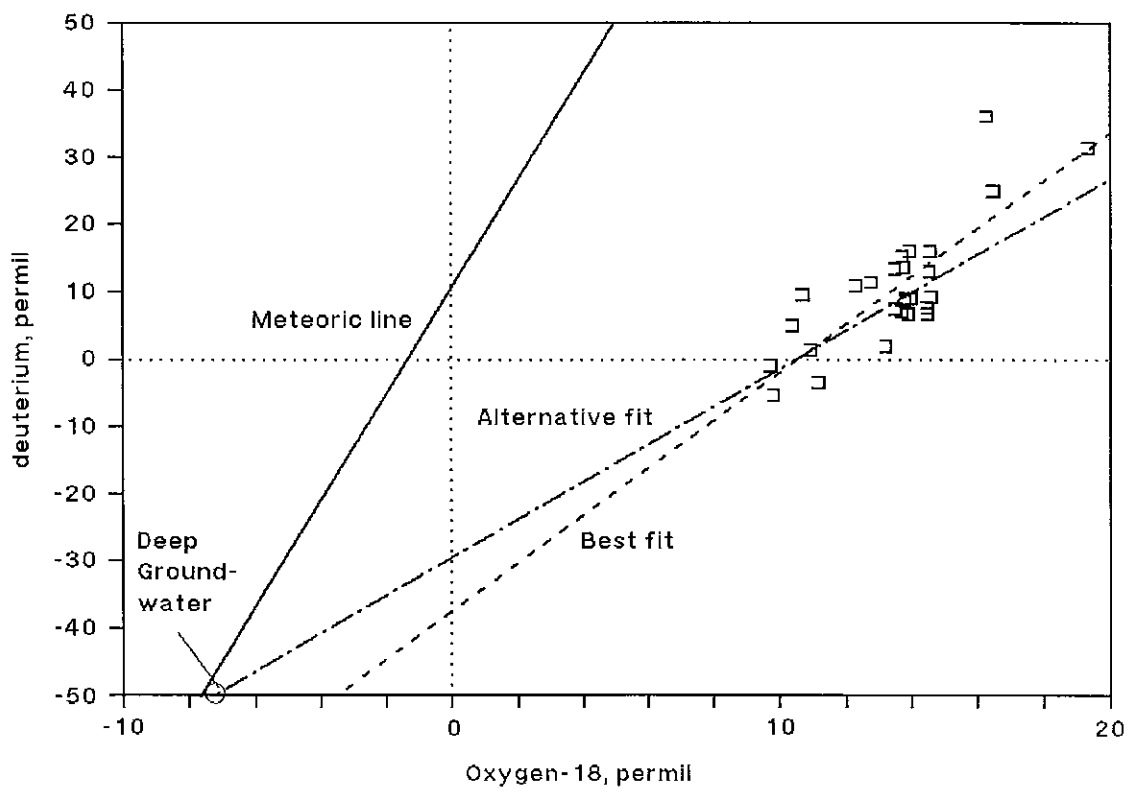


FIGURE 5.4.7 Hole 11 Pore Water ,O-18 - D Plot

compared to the equilibrium fractionation of 20‰ (Sofer, 1978; see section 2.1.2). Only a small number of gypsum water samples could be analysed for oxygen-18 in the time available, and these proved to be also depleted relative to pore waters at the same depth by an average of about 7.7‰, whereas at equilibrium the values would be enriched by 4‰. It is safe to conclude then that the gypsum is not in isotopic equilibrium with the (present day) coexisting pore waters.

For various samples from holes 10 and 11, gypsum crystal and associated pore waters are plotted in O-18 - D space in figure 5.5.1, together with the theoretical waters in equilibrium with the gypsum waters. The theoretical parent waters of the gypsum lie on the same "evaporation line" as the pore waters, but closer to the local GAB water.

This suggests that the gypsum was deposited by waters undergoing the same evaporative enrichment as the present day pore waters, but at a less concentrated stage.

One way this situation could come about is if the gypsum was deposited at greater depth below the surface than at present, where the pore water is less enriched, and now occurs closer to the surface due to erosion. This implies that the gypsum has been in place for some time, probably thousands of years. There are however inclusions of brown, weathered material in some of the gypsum crystals in most near-surface samples, which imply that the gypsum grew in place after fairly intense weathering had already taken place: the brown coloration usually only persists to a couple of metres depth.

Alternatively, the gypsum could have been deposited at its current position near the surface at an earlier time when the pore waters were less enriched because the present arid climate had not been in effect as long as now. The enrichment over such a large depth of soil and rock from production near the surface would be expected to build up slowly

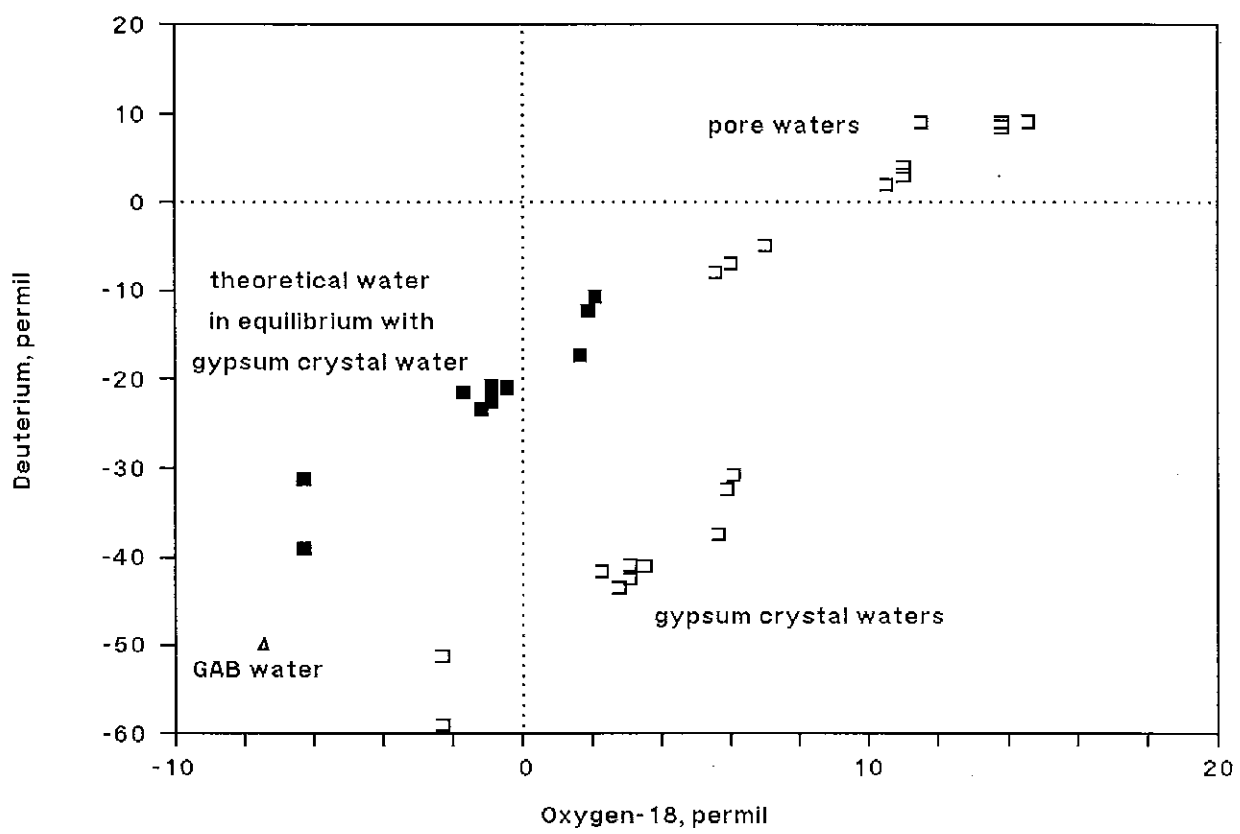


FIGURE 5.5.1 Relationship between gypsum crystal and pore waters, holes 10 and 11, O-18 - D Plot

from an initial state.

Even if the profiles have been changing very slowly over the last few millennia, this does not mean that the estimates of evaporation are invalid. The profiles beneath the evaporation front for steady-state and unsteady for the same instantaneous evaporation rates are very similar (Barnes & Allison, 1988), and the errors in taking an exponential model of the profile for an estimate of evaporation is small. As shown by Walker *et al.* (1988) and unpublished work of G.R. Walker, I.D. Jolly and the author (not presented), apart from early times an unsteady deuterium profile (and by association chloride, since it behaves similarly) changes slowly, being related to  $1/\sqrt{\text{time}}$ .

Gypsum veins were observed in the Bulldog Shale to depths of greater than 10m, and were usually much cleaner and clearer than those near the surface. Deuterium data from the deepest hole, 14, shows that the deeper gypsum veins are closer to being at equilibrium with the coexisting pore waters those than near the surface (fig. 5.5.2). Active gypsum precipitation is probably occurring at greater depth, as ongoing upward leakage brings with it the parent calcium and sulphate ions.

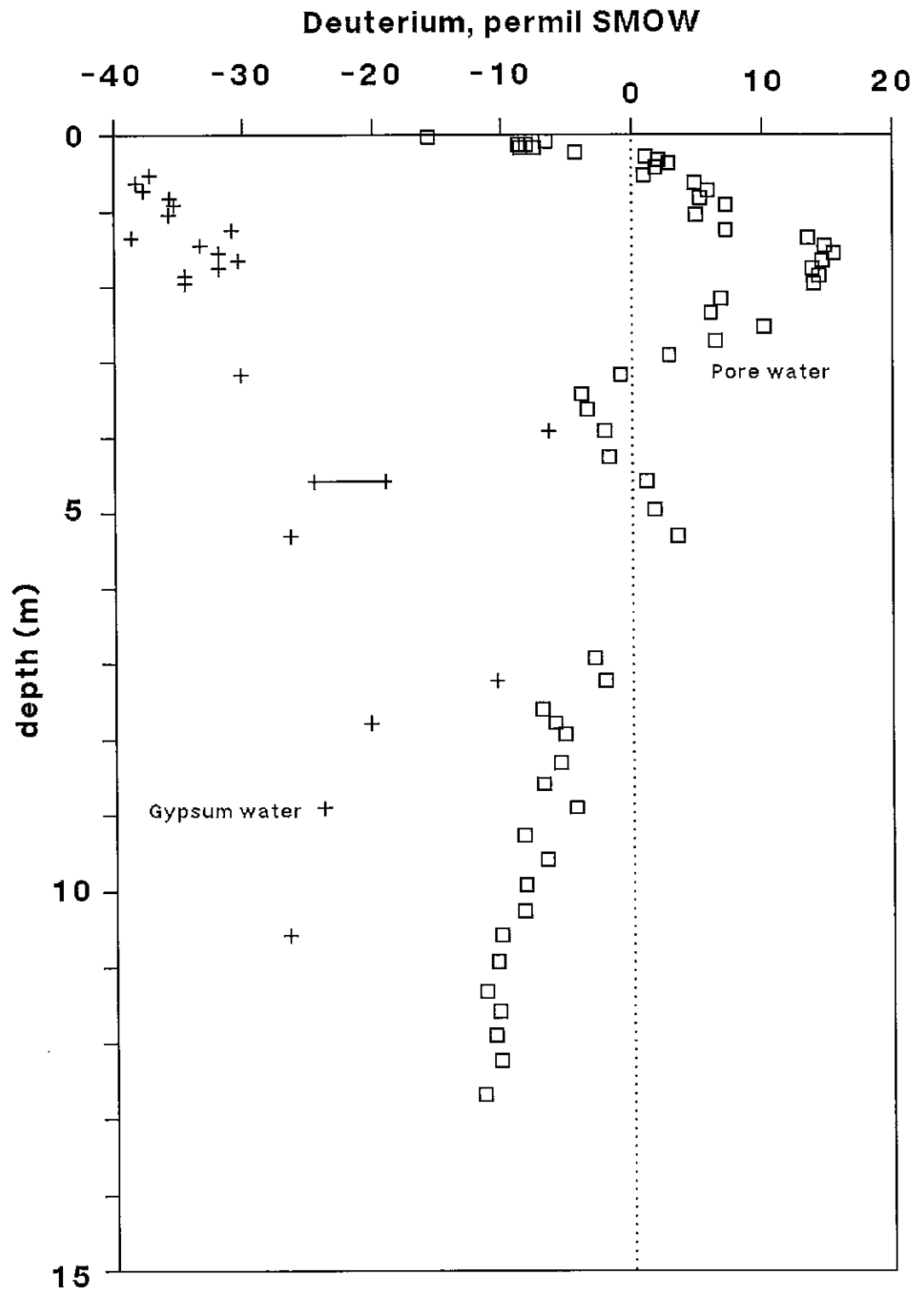


FIGURE 5.5.2 Deuterium profiles of gypsum and pore waters, hole 14